construction
engineering
research
laboratory

TECHNICAL REPORT M-217
May 1977
Corrosion Behavior of Cracked Fibrous Concrete

CORROSION BEHAVIOR OF STEEL FIBROUS CONCRETE

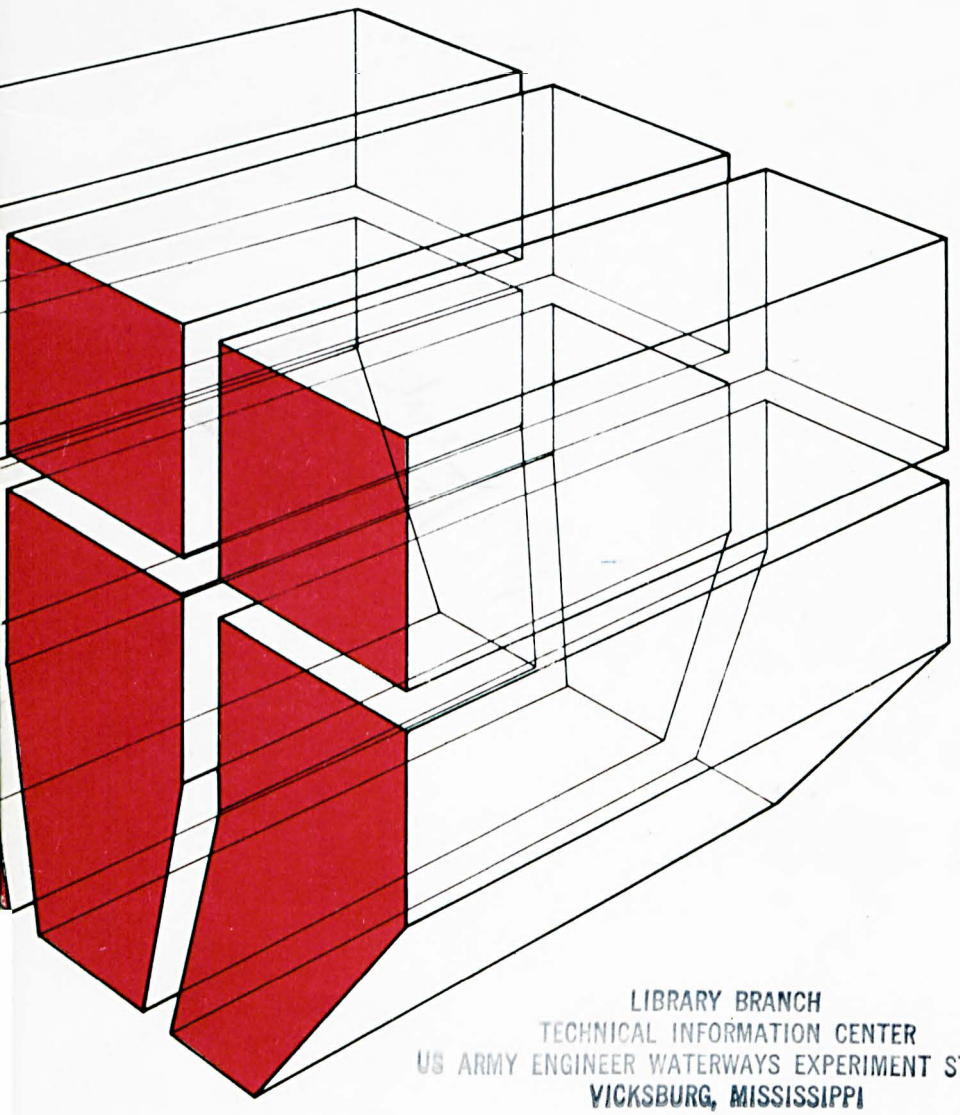

by
D. C. Morse
G. R. Williamson

SECURITY CLASSIFICATION OF THIS PAGE (When Data Entered)

REPORT DOCUMENTATION PAGE

READ INSTRUCTIONS BEFORE COMPLETING FORM

1. REPORT NUMBER: CERL-TR-M-217	2. GOVT ACCESSION NO.
3. RECIPIENT'S CATALOG NUMBER	
4. TITLE (and Subtitle): CORROSION BEHAVIOR OF STEEL FIBROUS CONCRETE	5. TYPE OF REPORT & PERIOD COVERED: FINAL
6. PERFORMING ORG. REPORT NUMBER	
7. AUTHOR(s): D. C. Morse G. R. Williamson	8. CONTRACT OR GRANT NUMBER(s)
9. PERFORMING ORGANIZATION NAME AND ADDRESS: CONSTRUCTION ENGINEERING RESEARCH LABORATORY P.O. Box 4005 Champaign, IL 61820	10. PROGRAM ELEMENT, PROJECT, TASK AREA & WORK UNIT NUMBERS: 4A7627T9AT41-T7-003
11. CONTROLLING OFFICE NAME AND ADDRESS	12. REPORT DATE: May 1977
	13. NUMBER OF PAGES: 36
14. MONITORING AGENCY NAME & ADDRESS (if different from Controlling Office)	15. SECURITY CLASS. (of this report): Unclassified
	15a. DECLASSIFICATION/DOWNGRADING SCHEDULE

16. DISTRIBUTION STATEMENT (of this Report)

Approved for public release; distribution unlimited.

17. DISTRIBUTION STATEMENT (of the abstract entered in Block 20, if different from Report)

18. SUPPLEMENTARY NOTES

Copies are obtainable from National Technical Information Service
Springfield, VA 22151

19. KEY WORDS (Continue on reverse side if necessary and identify by block number)

steel fibrous concrete
corrosion
cracked fibrous concrete

20. ABSTRACT (Continue on reverse side if necessary and identify by block number)

This report presents the results of an investigation into four aspects of the corrosion behavior of steel fibrous concrete:

1. The behavior of cracked and uncracked metallic and nonmetallic fibrous concrete subjected to a natural wet-dry, freeze-thaw saltwater environment

2. The effect of crack width on the corrosion of fibers bridging the crack

DD FORM 1 JAN 73 1473 EDITION OF 1 NOV 65 IS OBSOLETE

UNCLASSIFIED

SECURITY CLASSIFICATION OF THIS PAGE (When Data Entered)

Block 20 continued.

3. The effect of various durations of exposure to a corrosive environment on constant-crack-width and uncracked steel fibrous concrete specimens

4. The effect of fatigue.

Results indicate that good quality, air-entrained, uncracked steel fibrous concrete does not experience any undesirable strength changes when subjected to a seawater environment for up to 1.5 years. Results also indicate that unworking cracks less than 0.01 in. (0.25 mm) wide do not provide sufficient passageway for corrosive liquids to cause corrosion of the fibers bridging the crack, while fibers bridging larger cracks can be expected to corrode. The fatigue behavior of uncracked, good quality, air-entrained steel fibrous concrete at 65 percent of the first cracked stress level was found to be unaffected by exposure to a saltwater environment.

FOREWORD

This investigation was performed for the Directorate of Military Construction, Office of the Chief of Engineers (OCE) under Project 4A7627T9AT41, "Design, Construction and Operations and Maintenance Technology for Military Facilities"; Task T7, "Materials Research and Development for Military Construction"; Work Unit 003, "Corrosion Behavior of Cracked Fibrous Concrete." The applicable QCR is 1.03.007. The OCE Technical Monitor was Mr. S. S. Gillespie.

This study was conducted by the Construction Materials Branch (MSC) of the Materials and Science Division (MS), U. S. Army Construction Engineering Research Laboratory (CERL). CERL personnel involved in this investigation were Mr. D. C. Morse, Dr. D. Naus, Dr. G. R. Williamson, and Messrs. R. Neu, R. Lampo, J. Gambill, and K. Ryan.

Appreciation is expressed to Mr. H. Thornton and Mr. G. Harris of the Waterways Experiment Station for their help and cooperation.

Dr. G. R. Williamson is Chief of MS, and Mr. P. A. Howdyshell is Chief of MSC. COL J. E. Hays is Commander and Director of CERL and Dr. L. R. Shaffer is Technical Director.

CONTENTS

TABLES

FIGURES

FIGURES (Cont.)

CORROSION BEHAVIOR OF STEEL FIBROUS CONCRETE

1 INTRODUCTION

Problem

Fibrous concrete, which is concrete with short, finely divided and randomly distributed fibers added, provides a practical method for dealing with the low tensile strength and brittle nature of plain concrete. The advantages of fibrous concrete over plain concrete are increased tensile strength, improved ductility, and superior fatigue performance.[1] The extent to which these advantages are fulfilled depends largely on the type of fiber and the volume percentage contained in the mix.

The use of fibers to reinforce concrete is a relatively new concept. As with almost any new concept, although fibrous concrete provides solutions to some problems, other complications have arisen. At least three characteristics of fibrous concrete should be examined before it is considered for widespread use.

1. The ultimate strength of fibrous concrete occurs after visible cracking has occurred. When cracking occurs, fibers are exposed; these exposed fibers may be attacked by corrosion, depending on the fiber and/or crack width.

2. Fibers have a large amount of surface area per unit volume of fiber material. Increased surface areas tend to accelerate corrosion rates. Although the surrounding concrete is expected to provide some protection for the fibers, the adequacy of this protection is questionable.

3. Since fibrous concrete is a composite, with the reinforcement distributed uniformly throughout the material, fibers are likely to exist on or near the surface. Minimum cover specifications indicate that these fibers may be subject to corrosion.

It can be hypothesized that corrosion may have an impact on the performance of fibrous concrete, depending on the susceptibility of the particular type of fiber used. The considerable success experienced with use of steel fibers is largely due to the superior structural properties which they provide for the concrete. Although the conditions under which steel fibers corrode in steel fibrous concrete are yet to be determined, steel fibers are unfortunately expected to be highly suceptible to corrosion. Thus, research examining the corrosive conditions which affect the performance of steel fibrous concrete is needed.

Objective

The purpose of this study is to determine the conditions under which corrosion can affect steel fibrous concrete in the uncracked and post-cracking stages. This report describes the methods and results of four experimental investigations addressing specific aspects of corrosion behavior of fibrous concrete:

1. The behavior of cracked and uncracked metallic and nonmetallic fibrous concrete subjected to a natural wet-dry, freeze-thaw saltwater environment (Chapter 2)

2. The effect of crack width on the corrosion of fibers bridging the crack (Chapter 3)

3. The effect of various durations of exposure to a corrosive environment on constant-crack-width and uncracked steel fibrous concrete specimens (Chapter 4)

4. The effect of fatigue on the corrosion behavior of fibrous concrete (Chapter 5).

The results of these studies are discussed independently and interdependently.

Background

An understanding of the process of steel corrosion in concrete is essential to this study. Verbeck[2] points out that the factors which induce corrosion of steel imbedded in concrete are the presence of oxygen, chloride ions, carbon dioxide, and water.

Oxygen is necessary if steel is to corrode in the high-pH environment normal to concrete. Since the rate of oxygen reduction must equal the rate of steel oxidation, the availability of oxygen can control the rate of steel corrosion. Oxygen is available to fibrous concrete from the air or as a dissolved gas in liquids. The extent to which oxygen reaches steel imbedded in concrete

[1] G. R. Williamson and B. H. Gray, *Technical Information Pamphlet on the Use of Fibrous Concrete*, Preliminary Report M-44/AD761077 (U. S. Army Construction Engineering Research Laboratory [CERL], May 1973).

[2] G. J. Verbeck, "Mechanisms of Corrosion of Steel in Concrete," *Corrosion of Metals in Concrete*, Publication SP-49 (American Concrete Institute [ACI], 1975), pp 21-38.

depends on the permeability of the concrete, the depth of concrete cover, and the existence of cracks.

Although chloride ions affect the rate of steel corrosion in concrete, corrosion can occur without them. Verbeck has reported that steel subjected to a concrete environment normally develops a protective oxide film of which chloride ions appear to be specific and unique destroyers. Chlorides may be available to fibrous concrete from such sources as deicer salts, mixing water, and seawater exposure, and may reach imbedded steel by permeation, spalling due to recrystallization or freeze-thaw, or direct contact in cracked sections.

There appears to be a definite relationship between the rate of steel corrosion, pH, and chloride ion concentration. According to Verbeck, the works of Shalon and Raphael,[3] and Hausmann[4] suggest that there is a threshold concentration which must be exceeded before corrosion occurs. An increase in chloride ion concentration beyond this threshold concentration results in an increased rate of corrosion up to some limit. At this limit, the availability of oxygen necessary for corrosion to occur may be significantly reduced. Empirical data from prior research indicate that a chloride:hydroxyl ion molar activity ratio of approximately 0.6 in solution at the iron-paste interface is a probable threshold value.[5] At a pH less than 11.5, corrosion may occur without chlorides. At a pH greater than 11.5, a measurable amount of chloride is required; that amount increases as the pH of the iron-liquid interface increases.[6]

Because of the presence of calcium hydroxide, concrete normally provides an alkaline environment. This environment may be destroyed by continuous rinsing or leaching, electrochemical reactions involving chloride ions in the presence of oxygen, or carbonation. Carbonation is a somewhat slow process involving the reaction of carbon dioxide with calcium hydroxide.[7] The concrete structure deteriorates, and its alkalinity is neutralized. Carbon dioxide is abundant in the atmosphere and may also be found as a dissolved gas in liquids.

Corrosion of steel will not occur without water. Not only does water take part in the chemical reaction which changes iron to rust, it also provides a medium in which corrosion-producing factors can move. For example, water can carry dissolved oxygen, chlorides and carbon dioxide to steel imbedded in concrete. The extent to which the steel is exposed to these corrosion producers depends on the permeability of the concrete, the thickness of cover, and the existence of cracks.

Although permeability of fibrous concrete can be controlled to a certain degree, cracks can be expected to occur, and fibers do exist on or very near the surface. Thus, it likely that corrosion may diminish the properties which fibers provide to concrete. Before this hypothesis can be validated, however, the corrosive conditions which affect the performance of fibrous concrete must be determined.

Mode of Technology Transfer

Specifications for the use of steel fibrous concrete have yet to be incorporated into Corps of Engineers Guide Specification CE 204, *Concrete (For Building Construction)* and Military Construction Guide Specification MCGS 02611, *Concrete Pavement for Roads and Airfields*. The information in this report can be used as background information for the preparation of revision to the specifications. This information can also be used by project designers considering use of steel fibrous concrete.

2 BEHAVIOR OF FIBROUS CONCRETE SUBJECTED TO NATURAL WEATHERING

Introduction

Since actual weathering conditions are difficult to reproduce in the laboratory, natural weathering experiments are being conducted at Treat Island, located in Cobscook Bay near Eastport, ME. This severe exposure station, which is operated by the Waterways Experiment Station (WES), Vicksburg, MS, provides a wet-dry, freeze-thaw, saltwater environment. Exposure specimens can be installed at mean tide; the twice daily tide reversals and low air temperatures provide freeze-thaw conditions. The objective was to conduct dura-

[3] R. Shalon and M. Raphael, "Influence of Sea Water on Corrosion of Reinforcement," *ACI Journal*, Proceedings, Vol 55, No. 12 (June 1959), pp 1251-1268.

[4] D. A. Hausmann, "Steel Corrosion in Concrete," *Materials Protection* (November 1967), pp 19-22.

[5] B. Erlin and G. J. Verbeck, "Corrosion of Metals in Concrete–Needed Research," *Corrosion of Metals in Concrete*, Publication SP-49 (ACI, 1975), pp 39-46.

[6] Erlin and Verbeck.

[7] I. Biczok, *Concrete Corrosion and Concrete Protection* (Chemical Publishing Co., 1967).

bility studies at this location to evaluate the performance of cracked and uncracked metallic and nonmetallic fibrous concrete subjected to a wet-dry, freeze-thaw, saltwater environment over an extended time period.

Procedure

Five separate batches of fibrous concrete specimens were fabricated using the same basic mix design (Table 1). According to Lankard and Walker, from whom the mix proportions were obtained, this mix is typical of those used for various experimental overlay projects.[8] Each of the five batches contained a different type of fiber. Three batches contained steel fibers: 1 in. X 0.010 X 0.022 in. (0.25 mm X 0.25 mm X 0.56 mm) U. S. Steel chopped (Figure 1); 2 in. X 0.020 in. diameter (51 mm X 0.51 mm diameter) Bekaert crimped (Figure 2); and 2.5 in. X 0.025 in. diameter (64 mm X 0.64 mm diameter) Atlantic drawn (Figure 3). The remaining two batches contained nonmetallic fibers: 0.5 in. (13 mm) Kevlar (Figure 4); and 1 in. (25 mm) Fiberglas (Figure 5). Each batch was weighed to the nearest 0.1 lb (0.045 kg), and contained 1.5 percent by volume of the respective fibers.

The water-cement ratio was maintained at 0.5 for the various fiber mixes. Addition of a water-reducing admixture at the rate of 4 oz (118 cm^3) per sack of cement permitted use of a constant water-cement ratio despite the varying degrees of workability caused by the different fiber types. Table 2 shows the differences in workability as reflected by the slump measurements, along with air content determinations.

Fifteen specimens were fabricated for each batch: nine 3.5 in. X 4.5 in. X 16 in. (89 mm X 114 mm X 406 mm) beams and six 4 in. diameter X 8 in. (102 mm diameter X 203 mm) cylinders. The specimens were moist-cured under standard conditions in excess of 60 days to minimize strength gain due to concrete curing once the exposure of the moist corrosive environment was begun. After curing, all beams were tested for fundamental transverse frequency using American Society for Testing and Materials (ASTM) standard test method C 215-60. Three beams and six cylinders from each batch were used to determine flexural and compressive strengths according to ASTM C 39-72 and C 78-64, respectively. Six beam specimens per batch underwent exposure to the severe weathering. Of these, three were uncracked and three were cracked to different crack openings—hairline (less than 0.01 in. [0.25 mm]), 1/16 in. (1.6 mm), and 1/8 in. (3.2 mm). Stainless steel and brass identification tags were affixed to the ends of each specimen via expandable masonry screw anchors. The top, bottom, and sides of each beam group were photographed. The specimens were then packed in sawdust and foam underlay and sent to WES, where pulse velocity determinations were conducted. The specimens were repacked and sent to Treat Island, where they were installed in January 1975. The effect of the environment on the specimens was monitored using periodic transverse frequency and pulse velocity evaluations. In July 1976, one uncracked and all cracked specimens from each batch were returned to CERL for evaluation. Extended long-term exposure performance data will be obtained from periodic pulse velocity and resonant frequency determinations of the remaining two specimens per group.

The fibrous concrete specimens' performance after 1.5 years of exposure was evaluated by visual inspection of the outside surfaces and crack faces and flexural strength determinations. The cracked and uncracked specimens were examined, photographed, and tested for flexural strength according to ASTM C 39-72. Before and after flexural test data were compared, as were before and after visual appearances. The crack interfaces were photographed and examined for fiber corrosion.

Results

Table 2 summarizes test results for the Treat Island exposure specimens. It was found that the uncracked fibrous concrete continued to gain flexural strength during exposure to the moist corrosive environment due to more complete hydration. The strength increases for the uncracked Kevlar, Fiberglas, U. S. Steel, Bekaert, and Atlantic fibrous concrete specimens after 1.5 years' exposure to severe weathering were 1, 15, 16, 10, and 47 percent respectively. The longer fiber types tended to have greater strength increases. Figures 6 through 10 show the before and after visual appearances of each group of specimens. None of the cracked Kevlar fibrous specimens were returned in one piece, while two of the three cracked Fiberglas fibrous specimens were returned in one piece. The lack of significant concrete deterioration due to severe weathering can be attributed to the high cement factor typical of fibrous concrete mixes as well as the use of air entrainment. The outside surfaces of the steel fibrous concrete specimens exhibited brown surface staining due to

[8] D. R. Lankard and A. J. Walker, *Pavement Applications for Steel Fibrous Concrete*, presented at the ASCE Transportation Engineering Specialty Conference, Montreal, Canada, July 1974.

Table 1
Treat Island Exposure Specimen Mix Design

Mix	Fiber, lb/cu yd (kg/m^3)	Cement, lb/cu yd (kg/m^3)	Sand, lb/cu yd (kg/m^3)	3/8-in. (10 mm) Pea Gravel lb/cu yd (kg/m^3)	Water, lb/cu yd (kg/m^3)	Air Entraining Agent, oz/cu yd (cm^3/m^3)	Water Reducer, oz/cu yd (cm^3/m^3
Kevlar	40 (24)	752 (446)	1500 (890)	1000 (593)	376 (223)	12 (464)	32 (1238)
Fiberglas	73 (43)	752 (446)	1500 (890)	1000 (593)	376 (223)	12 (464)	32 (1238)
U.S. Steel	200 (119)	752 (446)	1500 (890)	1000 (593)	376 (223)	12 (464)	32 (1238)
Bekaert	200 (119)	752 (446)	1500 (890)	1000 (593)	376 (223)	12 (464)	32 (1238)
Atlantic	200 (119)	752 (446)	1500 (890)	1000 (593)	376 (223)	12 (464)	32 (1238)

Table 2
Treat Island Exposure Specimen Testing Summary

Specimen Fiber Type	Slump, in. (cm)	Air %	Compressive Strength lb/sq in. (N/cm^2)	Ultimate Flexural Strength, lb/sq in. (N/cm^2) ASTM C 39-72					Change in Dyn. E After 1.5 Years Exposure (Uncracked Specimens Only), %	Change in Pulse Velocity After 1.5 Years Exposure (Uncracked Specimens Only), %
				0 Year, Uncracked	1.5 Years, Uncracked	1.5 Years, Hairline Crack <0.1 in. (.25 mm)	1.5 Years, 1/16-in. (1.6 mm) Crack	1.5 Years, 1/8-in. (3.2 mm) Crack		
Kevlar	0 (0)	10	4530 (3123)	890 (614)	896 (618)	0	0	0	+6	+51
Fiberglas	1 (2.5)	8	4472 (3083)	794 (547)	906 (625)	401 (276)	0	NA*	+1	+60
U.S. Steel	8 (20.3)	3.5	7318 (5046)	1216 (838)	1410 (972)	987 (681)	594 (410)	234 (161)	+3	+64
Bekaert	0 (0)	4.5	6284 (4333)	1422 (980)	1559 (1075)	1831 (1262)	1344 (927)	704 (485)	+4	+56
Atlantic	7 (17.8)	2.5	6207 (4280)	1299 (896)	1907 (1315)	NA*	971 (669)	1115 (769)	+1	+64

*Data not available

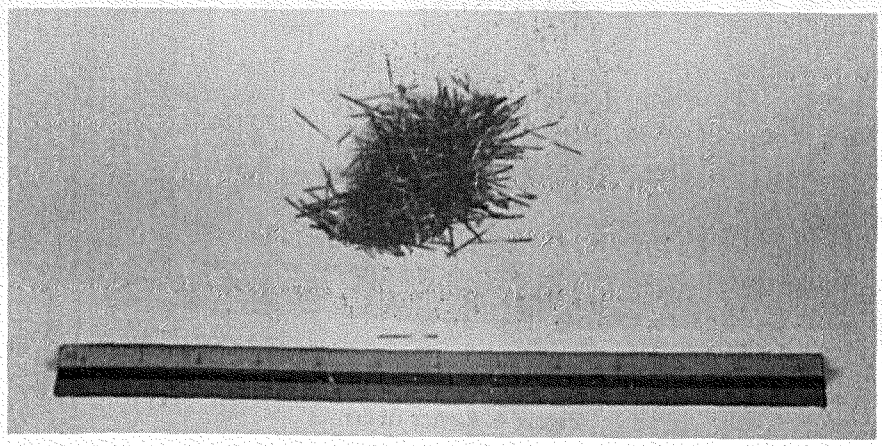

Figure 1. U.S. Steel fibers.

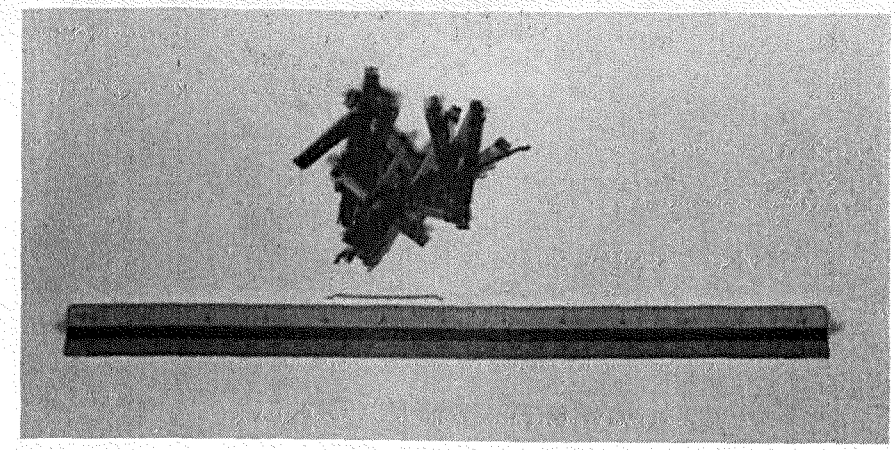

Figure 2. Bekaert fibers.

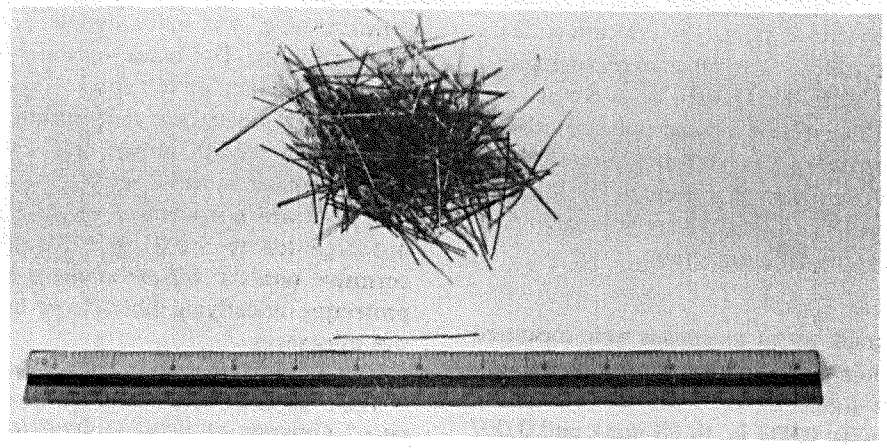

Figure 3. Atlantic fibers.

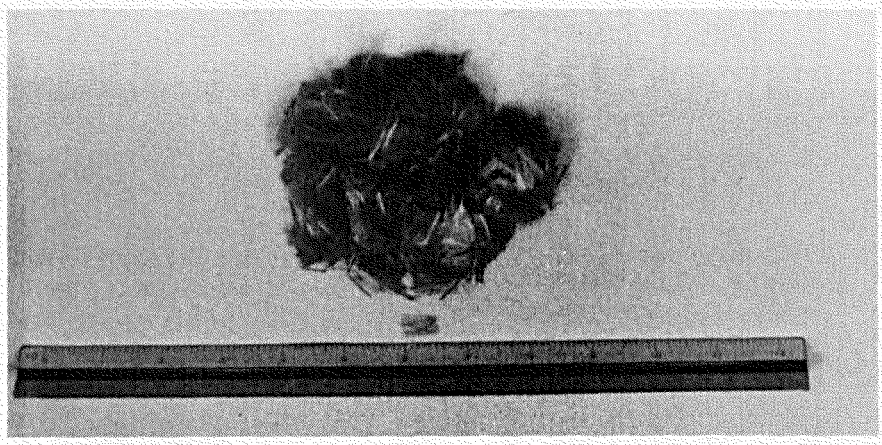

Figure 4. Kevlar fibers.

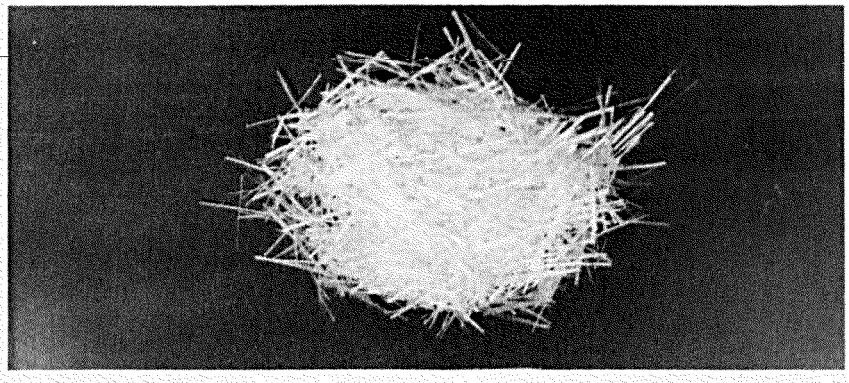

Figure 5. Fiberglas fibers.

corrosion of fibers on or very near the surface. Close examination of the fracture surfaces of the tested uncracked fibrous concrete specimens revealed no trace of corrosion of imbedded steel. The fracture surfaces of the specimens which were precracked to hairline (less than 0.01 in. [0.25 mm]), 1/16 in. (1.6 mm), and 1/8 in. (3.2 mm) crack widths showed evidence of fiber corrosion up to 1/8 in. (3.2 mm), 1 in. (25 mm), and 2 in. (51 mm) from the point of maximum crack width, respectively. Figures 11 through 15 are photographs of the crack interfaces of each beam group.

The hairline crack width specimens were measured for actual maximum crack width prior to flexural testing. Cracks were found to be 0.005 in. (0.13 mm), 0.008 in. (0.20 mm), 0.003 in. (0.08 mm), and 0.007 in. (0.18 mm) for the Fiberglas, U. S. Steel, Bekaert, and Atlantic specimens, respectively. No measurement was obtained for the hairline-cracked Kevlar specimen, since it was returned in two pieces. Some evidence of "crack sealing" was found during measurement of the hairline cracks. The crack openings were filled with corrosive product. It is expected that for small crack widths, steel fibers near the concrete surface corrode, producing a reddish brown corrosive product which "has a volume more than twice that of the metallic iron from which it was formed."[9] If the crack width is not large–less than 0.01 in. (25 mm)–enough of this corrosive product will be available to seal the crack, protecting underlying fibers from intrusion of corrosive substances.

[9]G. J. Verbeck, "Mechanisms of Corrosion of Steel in Concrete," *Corrosion of Metals in Concrete*, Publication SP-49 (ACI, 1975), pp 21-38.

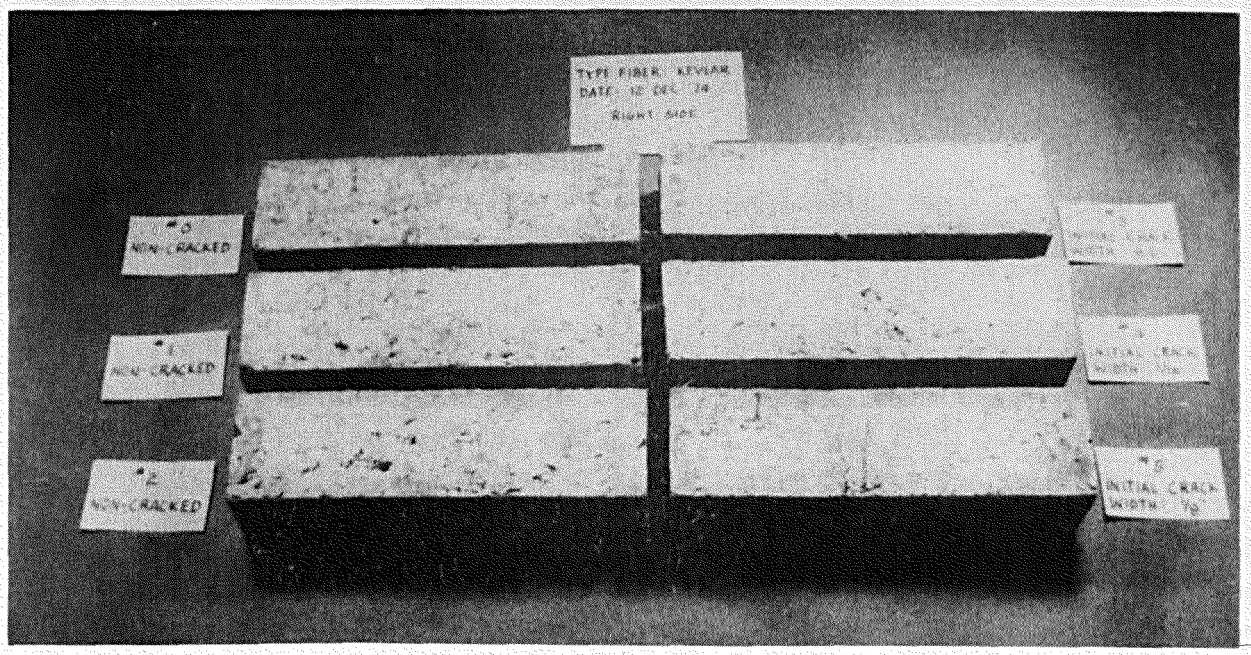

a. Before exposure.

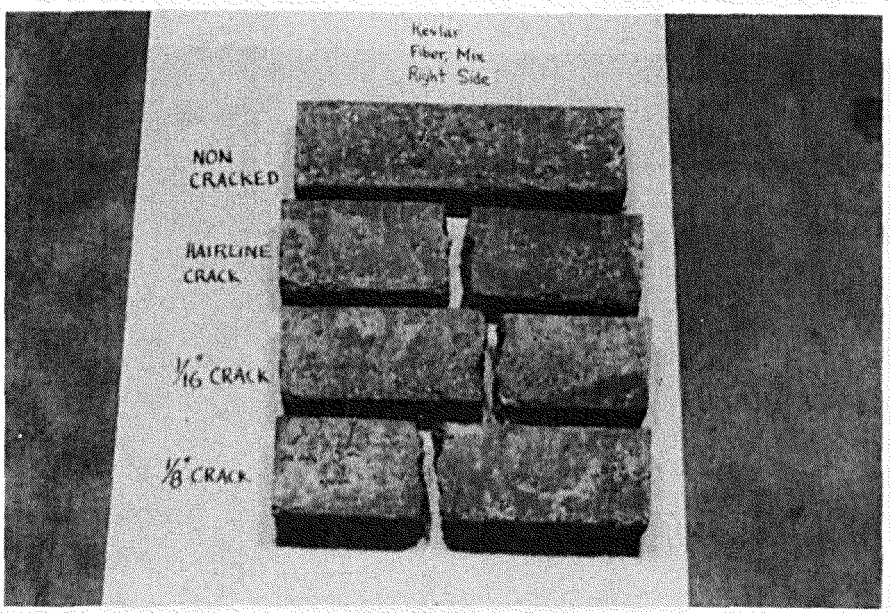

b. After exposure.

Figure 6. Kevlar specimens.

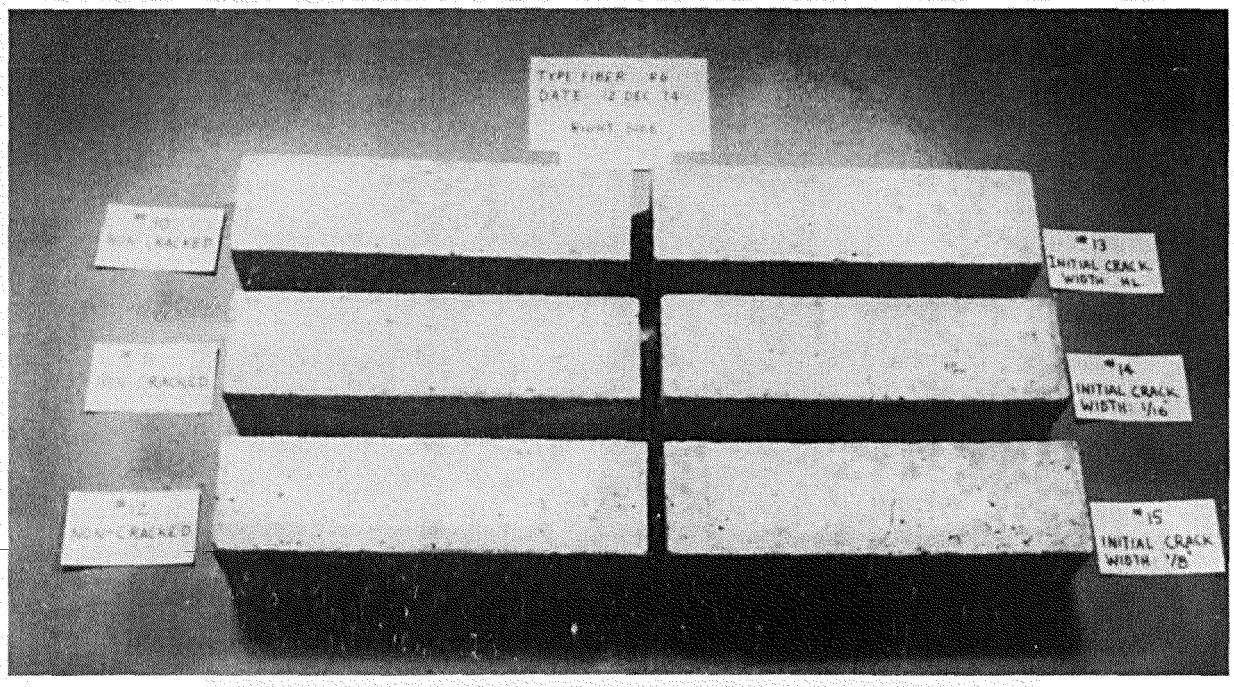

a. Before exposure.

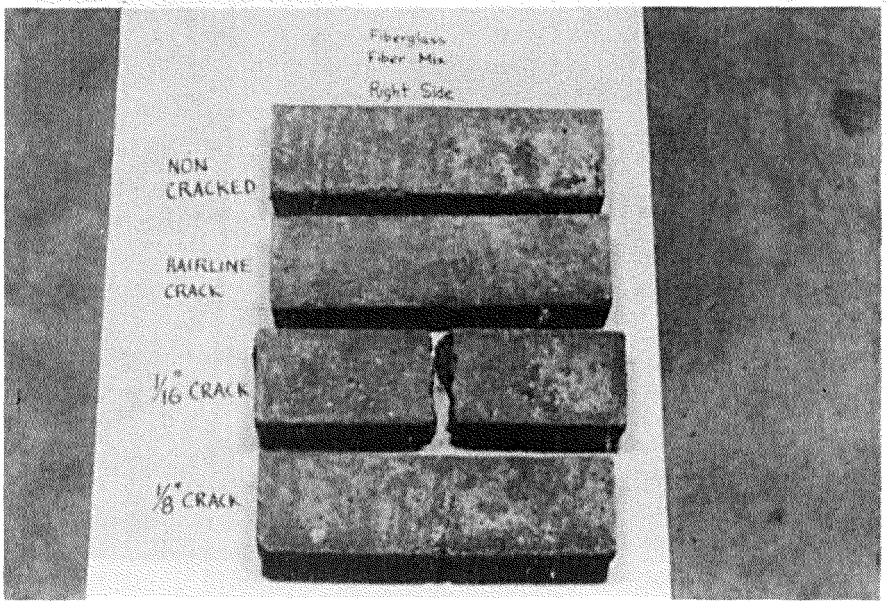

b. After exposure.

Figure 7. Fiberglas specimens.

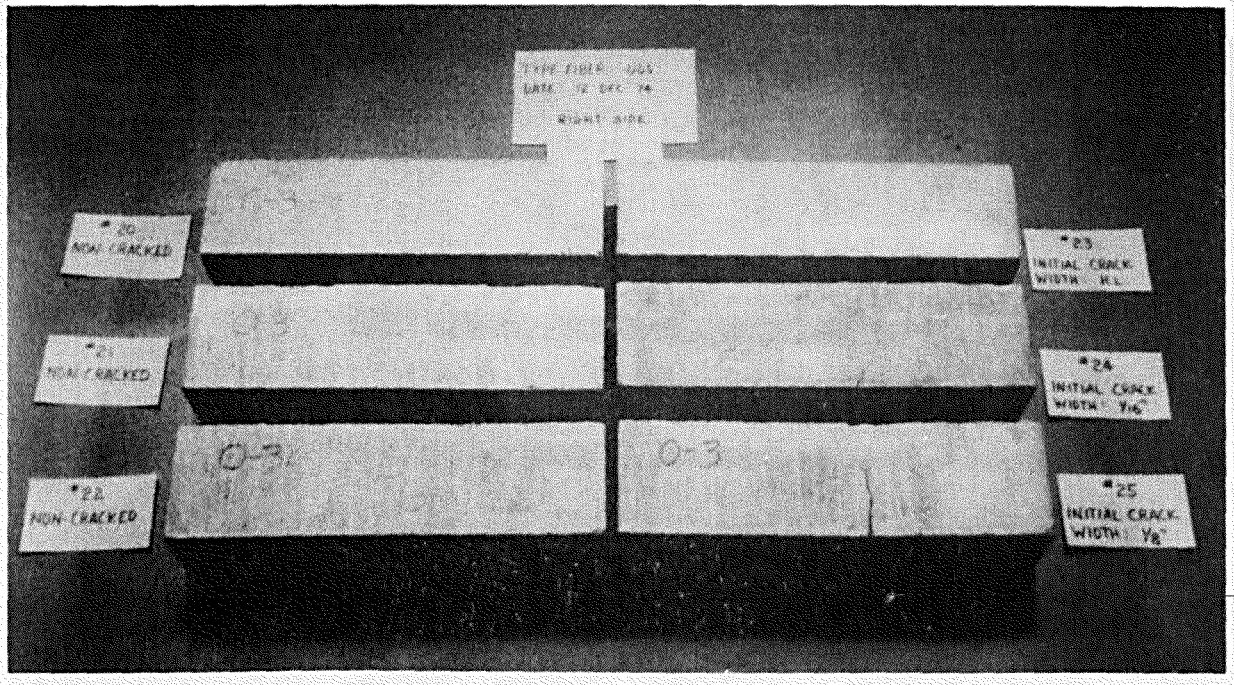

a. Before exposure.

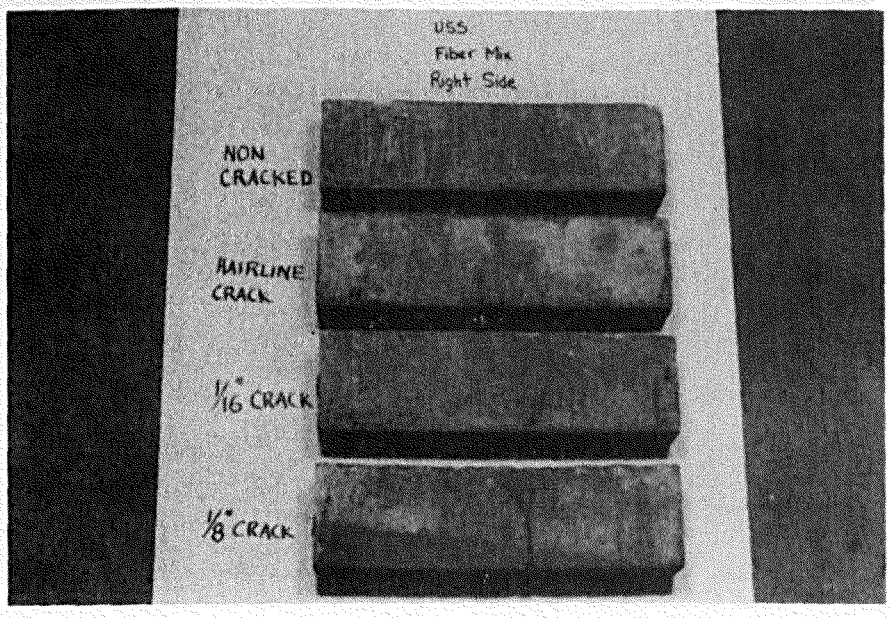

b. After exposure.

Figure 8. U. S. Steel specimens.

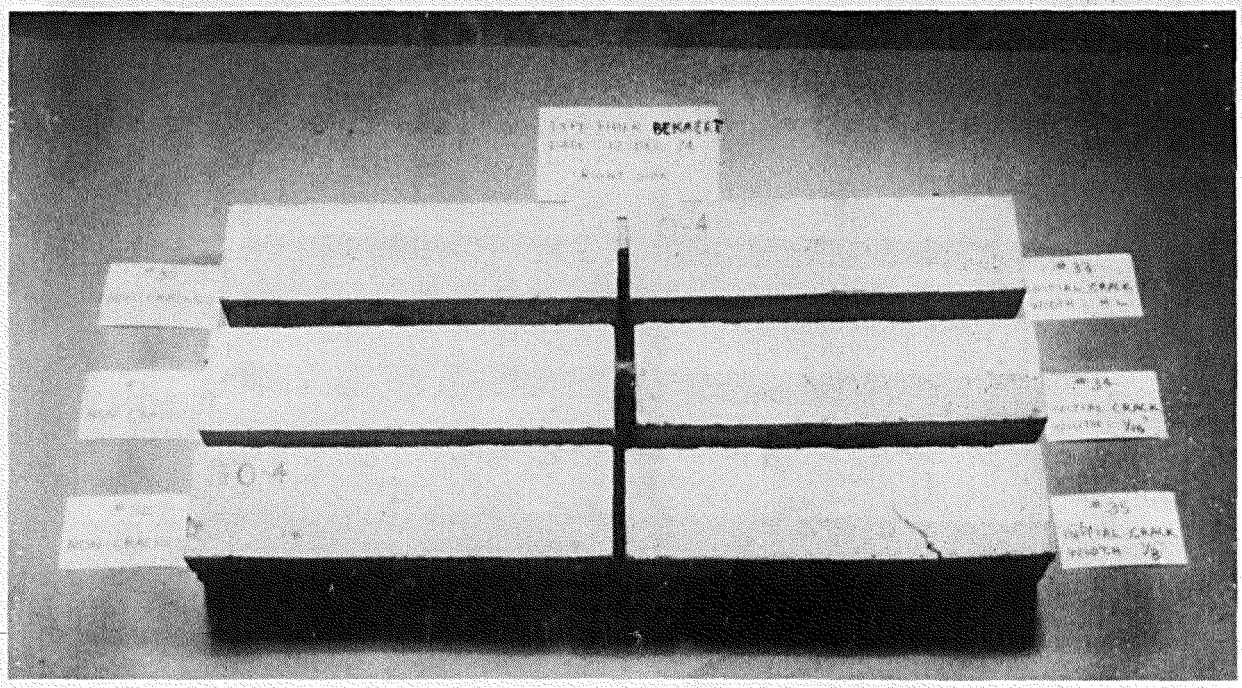

a. Before exposure.

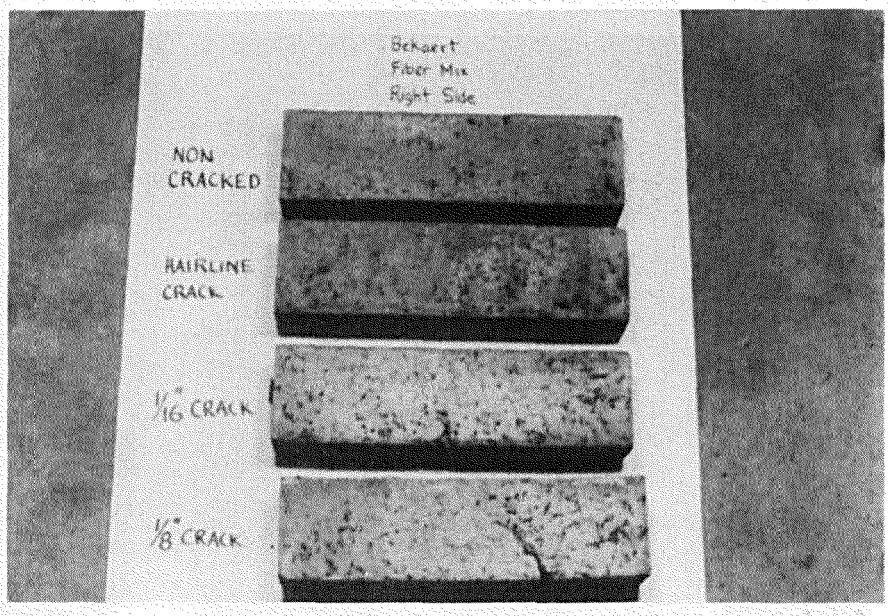

b. After exposure.

Figure 9. Bekaert specimens.

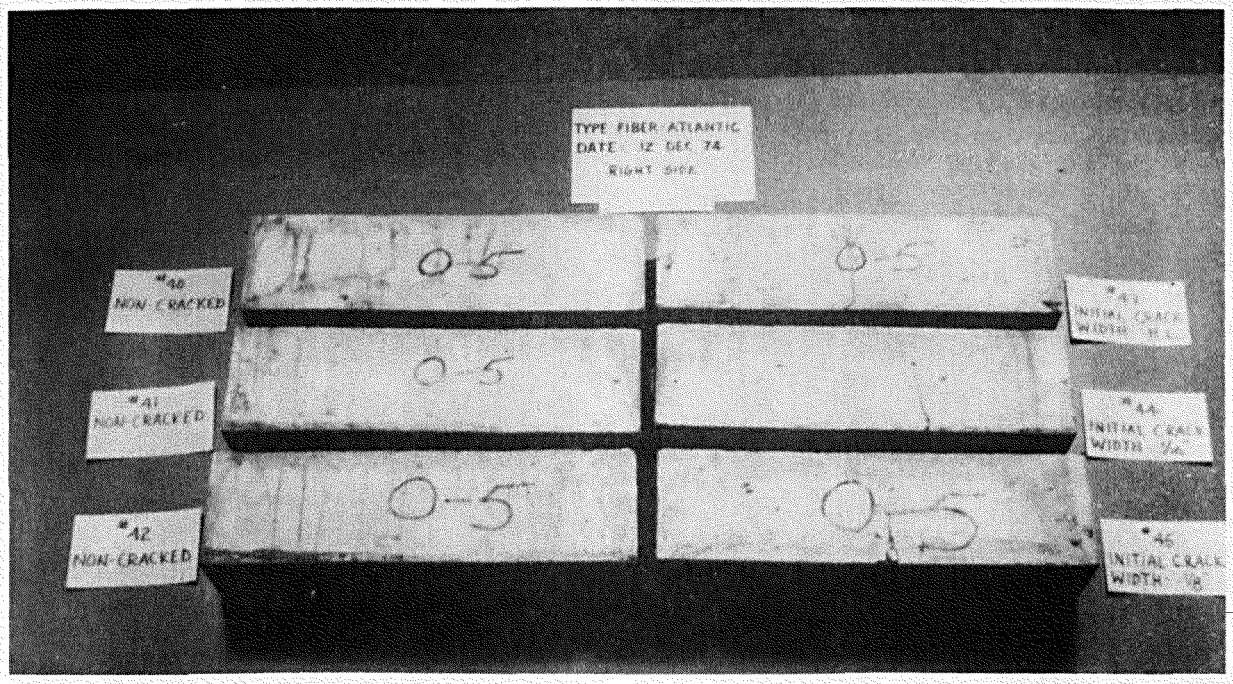

a. Before exposure.

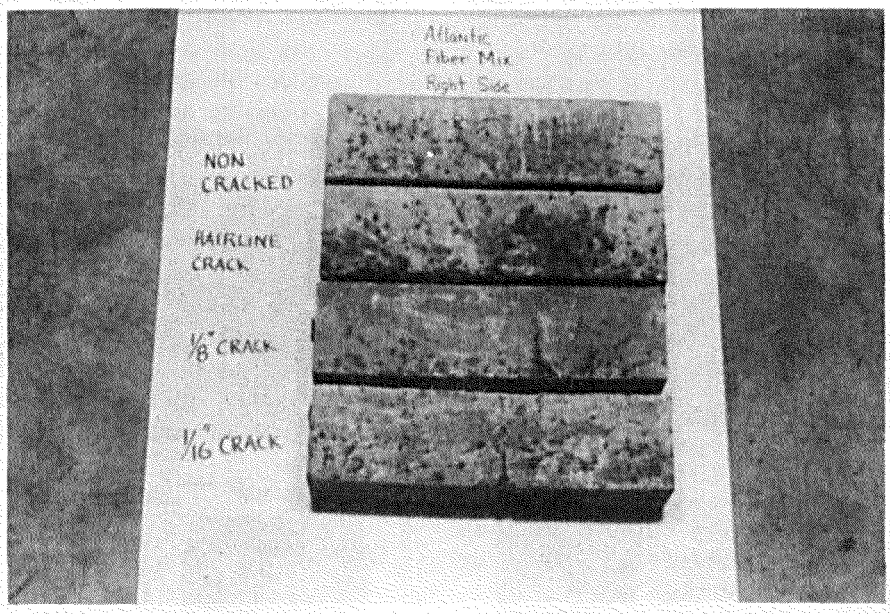

b. After exposure.

Figure 10. Atlantic specimens.

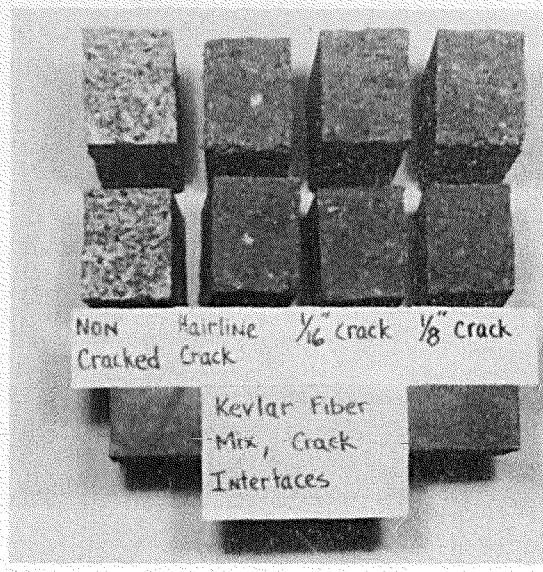

Figure 11. Kevlar specimen crack interfaces.

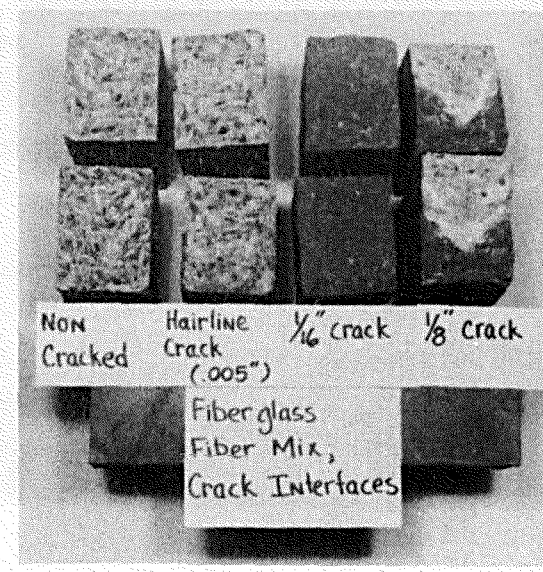

Figure 12. Fiberglas specimen crack interfaces.

Figure 13. U. S. Steel specimen crack interfaces.

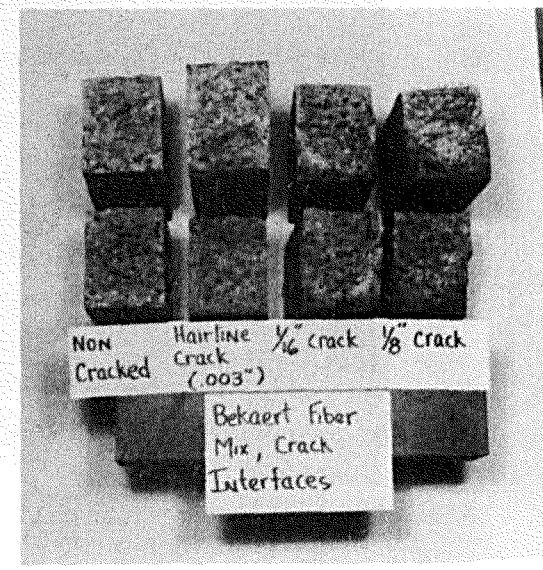

Figure 14. Bekaert specimen crack interfaces.

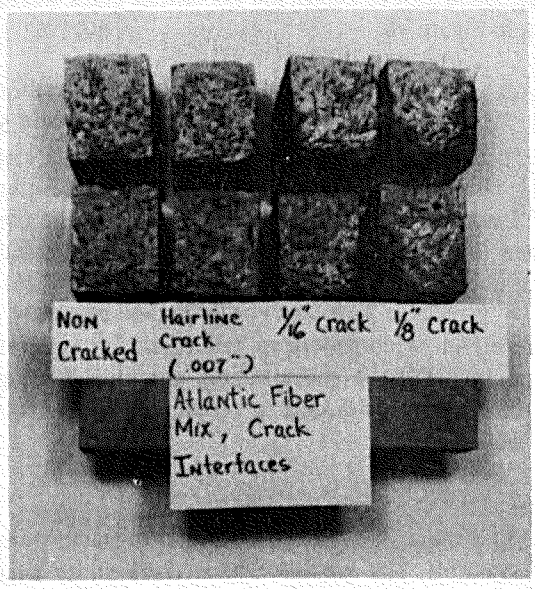

Figure 15. Atlantic specimen crack interfaces.

Discussion of Results

The results of this investigation show that uncracked and hairline-cracked fibrous concrete and uncracked nonmetallic fibrous concrete are not significantly affected by 1.5 years of exposure to severe natural weathering. The steel fibrous specimens precracked to 1/16-in. (1.6 mm) and 1/8-in. (3.3 mm) maximum crack openings experienced significant crack-bridging fiber corrosion. Very little can be said about the performance of the cracked Fiberglas and Kevlar fibrous concrete subjected to severe weathering, since these specimens exhibited low post-cracking ductility. It is expected that most of the damage to these specimens resulted from handling and shipping. Although the nonmetallic fibers were expected to be superior to the metallic fibers in corrosion resistance, this potential has very little meaning, since the nonmetallic fibrous concrete had relatively low post-cracking strength and ductility compared to the metallic fibrous concretes.

3 EFFECT OF CRACK WIDTH ON CORROSION BEHAVIOR OF CRACKED STEEL FIBROUS CONCRETE

Introduction

The fibers in fibrous concrete provide a considerable amount of post-cracking ductility. Ultimate flexural strength is attained in the post-cracking stage. However, it is hypothesized that a crack can expose bridging fibers to available corrosion-producing substances. It is also expected that the extent to which crack-bridging fibers are exposed depends somewhat on the crack width and the distance of the fiber from the concrete surface.

Typical fibrous concrete crack interfaces are highly irregular because fibrous concrete is a composite—strong and weak particles are mixed together. Cracks usually start at a highly stressed weak particle and continue in a straight line until they encounter a strong particle; crack direction may then change, seeking the path of weakest resistance. This change of crack direction is caused by both particle strength and orientation. The random distribution of the fibers may create weak alleys in which the overlapping distance of adjacent fibers may be inadequate. The constantly changing direction of fibrous concrete cracks coupled with the existence of sufficiently small crack widths could be a potential crack-bridging steel-fiber-corrosion-inhibiting mechanism for the following reasons:

1. Corroding steel produces a corrosion product which occupies a larger volume than the steel from which it was derived. This corrosive product, due to its expanding nature, is forced into the space between the interlocked crack interfaces. This occurrence could effectively seal in a high-pH environment as well as seal out excessive amounts of oxygen, thus promoting steel passivity.

2. The complexity and size of a steel fibrous concrete crack could greatly impede the flow of corrosive substances into and out of the cracked section. If the flow impedance is great enough, it could effectively reduce the corrosion rate to a near negligible value.

3. The flow impedance mentioned above could also support a passivating effect on the steel, since reduction of pH in a concrete environment is primarily caused by a large amount of nonalkaline substances flowing through the crack and rinsing out calcium hydroxide. Since flow is greatly impeded, a high-pH environment may be maintained, thus providing the conditions under which steel passivation will occur.

As crack width increases, the extent to which these events occur is expected to decrease until some maximum crack width is attained; at this width, crack-bridging fibers are no longer protected. The objective of the investigation described in this chapter is to

determine what the limiting crack width is and how it compares with those found in steel fibrous concrete being stressed at or near ultimate flexural stress.

Procedure

Seven 3.5 in. X 4.5 in. X 16 in. (89 mm X 114 mm X 406 mm) steel fibrous concrete flexure specimens were fabricated using the mix design shown in Table 3. Flexural cracks were produced in six of the specimens with a 500-kip (2.2 MN) Satec Universal Testing Machine. The crack width varied from about 1/16 in. (1.6 mm) at the extreme tension fiber to zero at about 5/8 in. (16 mm) from the extreme compression fiber.

The specimens were subjected to a corrosive environment consisting of alternate wetting and drying of a 3.5 percent sodium chloride solution. A flowing stream of saltwater was directed into the crack 8 hours per day for 30 days. The specimens were then removed from the environment for evaluation.

The crack width was measured using a calibrated illuminated surface microscope. Crack widths were measured along the depth of the beam at various distances from the bottom of the beam. From these data, a plot of crack width vs distance from extreme tension fiber was developed (Figure 16). The beams were then broken into two pieces to examine the crack interfaces. A boundary line was made on the crack interface to separate corroded from noncorroded fiber areas (Figure 17). The distance from this boundary at the center and edges of the crack interface to the bottom of the beam was measured. These data were used with the previously mentioned plot to determine the critical crack width shown in Figure 16.

To determine the stress crack width relationship of the 1.5 percent steel fibrous concrete, a 3.5 in. X 4.5 in. X 16 in. (89 mm X 114 mm X 406 mm) beam was loaded in 500-lb (2225 N) increments using center point loading. The crack width was measured at the extreme tension fiber with the calibrated illuminated surface microscope for each load increment.

The effect of corrosion on this particular type of cracked steel fibrous concrete was determined using the critical crack width data in conjunction with stress crack width data.

Results

Table 4 shows the results of the critical crack width determinations. The average critical crack width near the crack face edge was found to be 0.01 in. (0.25 mm). Assuming linear crack width distribution across the crack face, it was found that the critical crack width near the center of the crack face was 0.015 in. (0.38 mm). Variation between edge and center determination could be caused by either (1) the fibers near the center of the crack face were less accessible to the corrosive environment due to the complex nature of the fracture surface of the steel fibrous concrete and/or (2) the assumption of linear crack width distribution across the crack face was incorrect. Determining the relative significance of these two factors is difficult. However, if fibers near the crack edge are affected by corrosion, the subsequent strength loss increases crack widths,

Table 3
Standard 1.5 Percent Steel Fibrous Concrete Mix Design

Constituent	Amount per Cu Yd (per m^3)
Cement, Type 1 Portland	752 lb (446 kg)
River Sand, Specific Gravity = 2.65	1354 lb (803 kg)
Pea Gravel, 3/8 in. (10 mm) maximum Specific Gravity = 2.65	1354 lb (803 kg)
Steel Fiber, 1 in. X 0.01 in. X 0.022 in. (25 mm X 0.25 X 0.56 mm)	200 lb (119 kg)
Water, w/c = 0.5	376 lb (223 kg)
Water Reducer, Plastiment, Sika Chem. Co.	48 oz (1857 cm^3)
Air-Entraining Agent, Sika Chem. Co.	32 oz (1238 cm^3)

Table 4
Results of Critical Crack Width Study

Specimen No.	Maximum Crack Width, in. (mm)	Critical Crack Width Near Edge of Crack Face, in. (mm)	Critical Crack Width in Center of Crack Face, in. (mm)
1	0.058 (1.5)	.010 (.25)	.019 (.48)
2	0.069 (1.8)	.010 (.25)	.015 (.38)
3	0.120 (3.0)	.009 (.23)	.012 (.30)
4	0.063 (1.6)	.009 (.23)	.015 (.38)
5	0.061 (1.5)	.009 (.23)	.012 (.30)
6	0.040 (1.0)	.011 (.28)	.015 (.38)
	Average	.010 (.25)	.015 (.38)

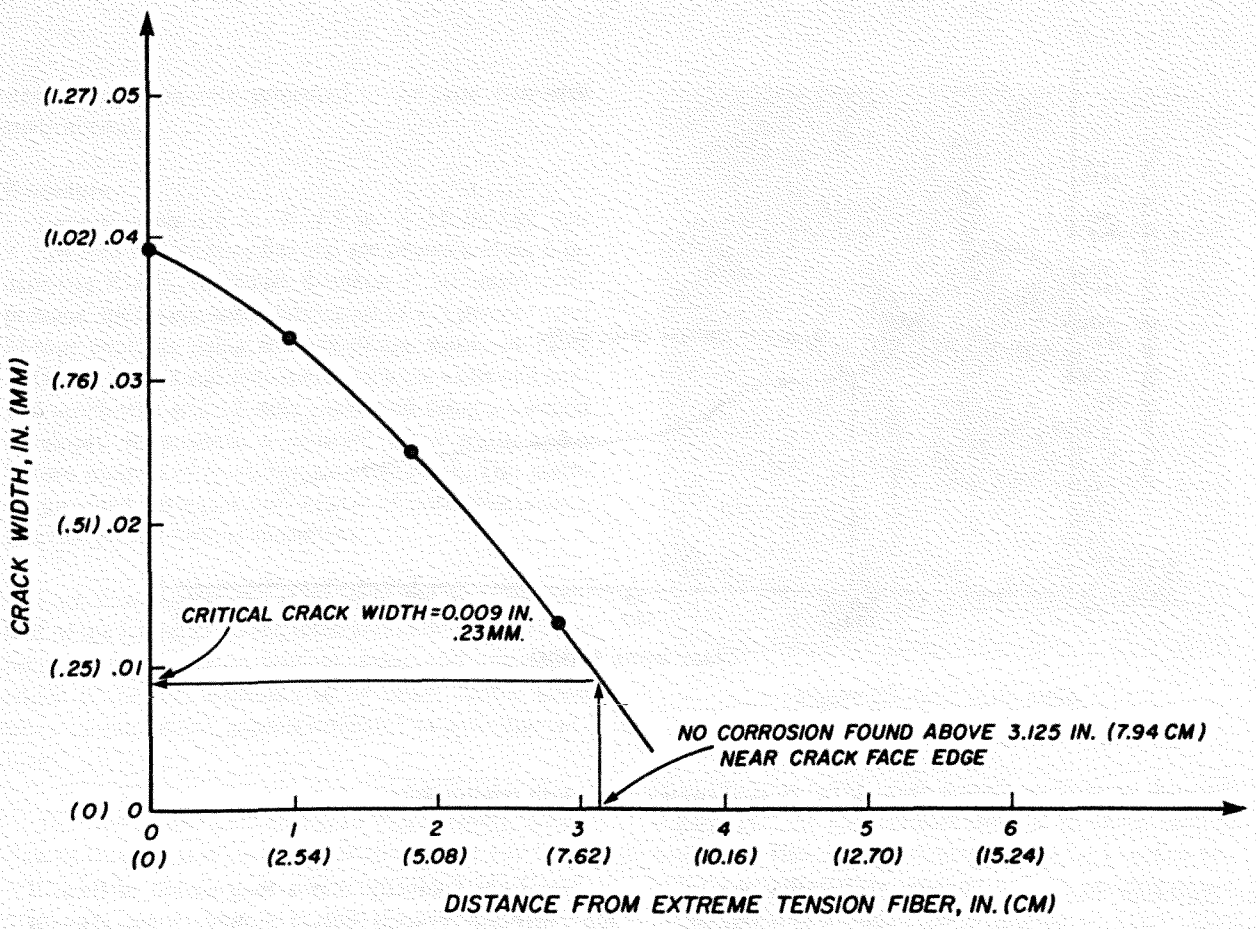

Figure 16. Typical crack width variation.

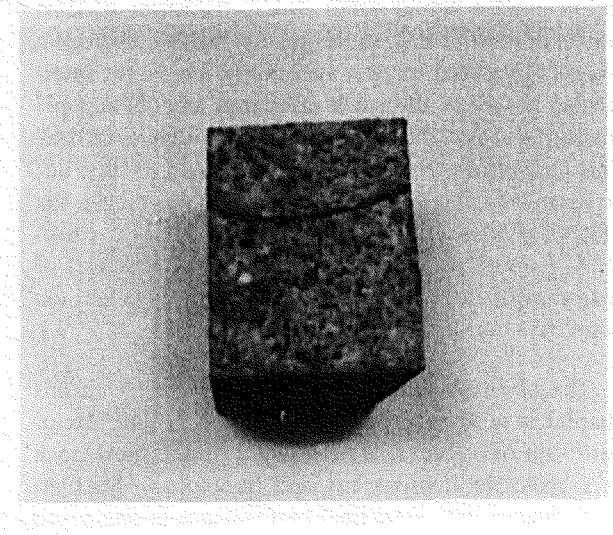

Figure 17. Corroded/noncorroded boundary line.

thus causing interior fibers to be corroded as well. Therefore, knowing the critical crack width at the crack face edge is more important, and the 0.01 in. (0.25 mm) value should be considered the absolute critical crack width.

Figure 18 shows the results of the stress vs. crack width test. It is apparent from this plot that at crack widths of 0.01 in. (0.25 mm), the 1.5 percent steel fibrous concrete is at a stress level of approximately 58 percent of the ultimate flexural strength, the ultimate strength having been reached at a crack width of approximately 0.0025 in. (0.06 mm).

Discussion of Results

Results of this investigation indicate that steel fibrous concrete of the type used in this study can be stressed at or near ultimate flexural strength without any major threat of widespread crack-bridging steel fi-

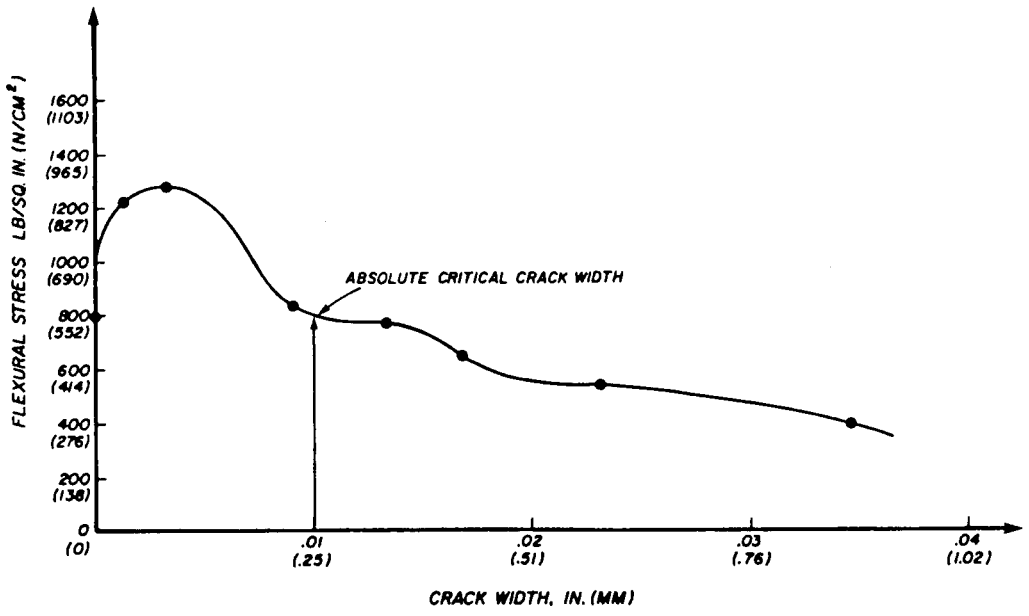

Figure 18. Typical stress-crack width relationship.

ber corrosion due to accompanying hairline cracks. However, if crack widths in steel fibrous concrete exceed 0.01 in. (0.25 mm), some form of protection should be provided to maintain integrity of the steel fibers bridging such cracks.

Results also indicate that steel fibers bridging a crack and existing near the center of the crack face are less vulnerable to corrosion than those bridging fibers near the edge of the crack face.

4 CORROSION RATE OF CONSTANT-CRACK-WIDTH AND UNCRACKED STEEL FIBROUS CONCRETE

Introduction

The investigation described in Chapter 3 indicated that steel fibers which bridge a large crack width (greater than 0.01 in. [0.25 mm]) are vulnerable to corrosive environments. How vulnerable these fibers are must still be determined. In addition, individuals responsible for maintaining in-service steel fibrous concrete must know whether loss of bridging-fiber integrity occurs quickly or progresses gradually over a long period of time. If the corrosion process occurs slowly, some type of cracked steel fibrous concrete corrosion inhibition program may be employed to preserve the strength which bridging fibers impart to cracked fibrous concrete. If the corrosion process occurs very quickly after critical crack width occurrence, the severely cracked section should be replaced. Because of the high surface area to volume ratio of steel fibers, it is expected that the corrosion process would occur rapidly. However, at least two conditions could cause greatly reduced corrosion rates: (1) reduced oxygen availability due to the interlocking nature of the crack interfaces, and (2) high-pH environment provided by the surrounding concrete. This high-pH environment is more difficult to rinse out in narrow and complex cracks, thus reinforcing the protective quality of the oxide coat described in Chapter 1. Experimental data which define the time rate of corrosion of steel fibers imbedded in concrete and exposed to a corrosive environment are needed.

The objective of the investigation described in this chapter is to experimentally determine the time rate of corrosion of a steel fiber in a larger than critical crack in a corrosive environment, and to compare this fiber performance with steel fiber performance in uncracked

steel fibrous concrete subjected to the same corrosive environment.

Procedure

Twenty-seven 3.5 in. X 4.5 in. X 16 in. (89 mm X 114 mm X 406 mm) flexural specimens and six 4 in. diameter X 8 in. (102 mm diameter X 203 mm) compression specimens were fabricated of 1.5 percent steel fibrous concrete using the mix design shown in Table 3. Of the 27 flexural specimens, 15 were unflawed control specimens and 12 were preflawed using a method developed to produce a constant crack width and a known number of fibers bridging this crack. This method provided for exact duplication of corrosion characteristics among various specimens.

Each flaw was located at midspan and occupied one-half of the lateral cross-sectional area. The flaw area was bounded by the beam bottom, sides, and mid-depth, which is the area expected to be under tensile stress when an uncracked beam is subjected to a positive moment.

The flaw width used was 1/16 in. (1.6 mm), since a flaw of this size is expected to totally expose any fibers which bridge the flaw. In addition, 1/16 in. (1.6 mm) cracks are not uncommon in severely cracked, shear-resistant steel fibrous concrete.

The preflawed specimens were produced using a grid plate (Figure 19) and grid plate puller (Figure 20). Both sides of the grid plate were covered with unidirectionally nylon-reinforced tape. The tape's reinforcement was oriented parallel to the slots in the grid plate. The plate was then pierced with one hundred and four 2.5 in. X 0.025 in. diameter (64 mm X 0.64 mm diameter) steel fibers at 0.025-in. (6.4 mm) spacings, as shown in Figure 21. The approximate number of fibers used to bridge the flaw was determined using Eq 1, which provides a statistical approximation of the number of unidirectionally oriented fibers which exist in a given cross section of the fibrous concrete.

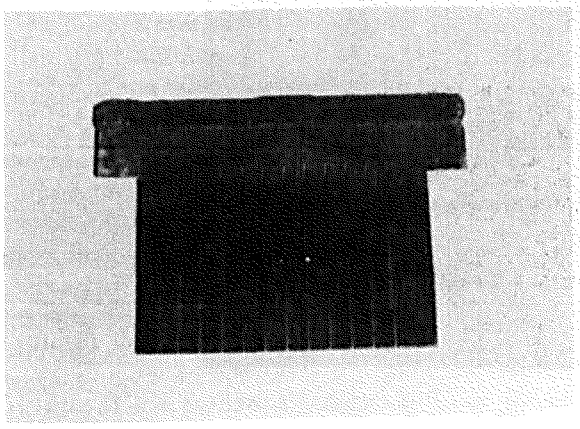

Figure 19. Grid plate.

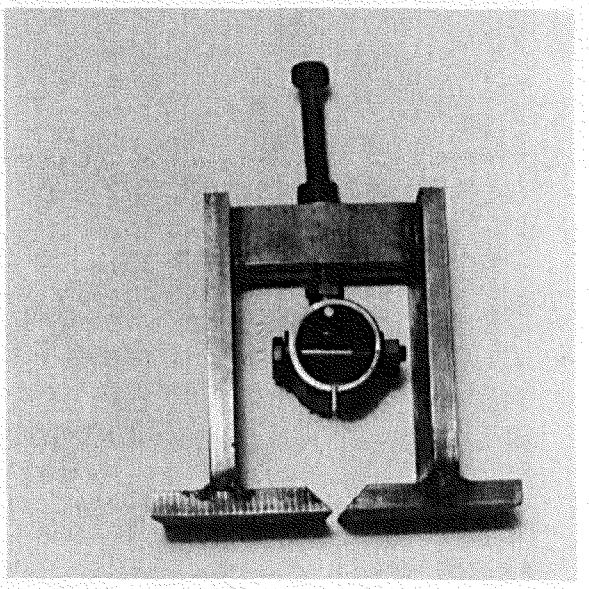

Figure 20. Grid plate puller.

$$N = \frac{A \cdot 41p}{a} \qquad \text{[Eq 1]}$$

where N = the number of unidirectional fibers in the flaw

A = the area of the flaw

p = the volume ratio of steel to concrete

a = the cross-sectional area of one fiber

.41 = a statistically determined orientation factor.[10]

For the given conditions (p equals .015), Eq 1 yields a value of 99. For simplicity and symmetry, a total of 104 fibers at 0.25-in. (6.4 mm) spacings were used to bridge the flaw.

[10]R. N. Swamy and P. S. Mangat, "A Theory for the Flexural Strength of Steel Fiber Reinforced Concrete," *Cement and Concrete Research*, Vol 4 (1974), pp 313-326.

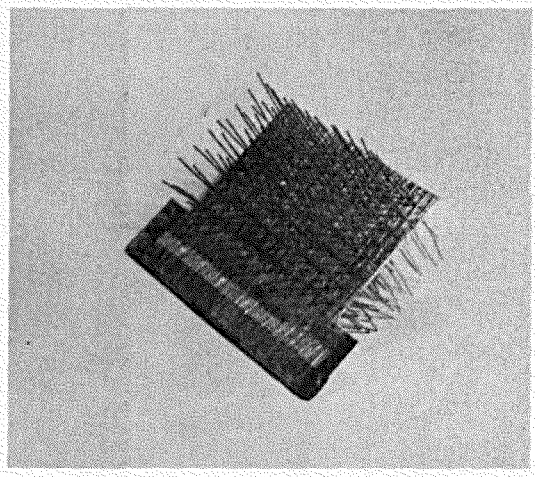

Figure 21. Grid plate with tape and fibers.

Once the fibers were uniformly distributed throughout the grid plate area, the resulting assembly was placed in the beam mold, which was then filled with plastic 1.5 percent steel fibrous concrete. Intermittent vibration was used to properly consolidate the concrete around the grid plate assembly. After 24 hours, the grid plate was removed from the specimen with the mold intact, as shown in Figure 22. The mold was then removed and the resulting preflawed steel fibrous concrete specimen (Figure 23) was ready for curing.

All specimens were cured for 28 days. The preflawed specimens were cured using a moisture barrier technique to prevent premature corrosion of the bridging fibers. The unflawed specimens were moist cured under standard conditions. Compression tests were conducted after the curing was completed.

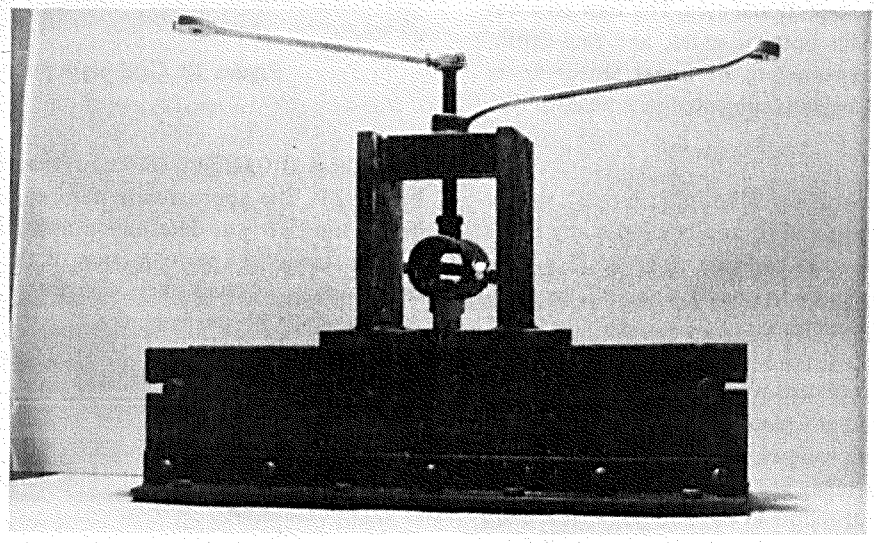

Figure 22. Removal of grid plate from specimen.

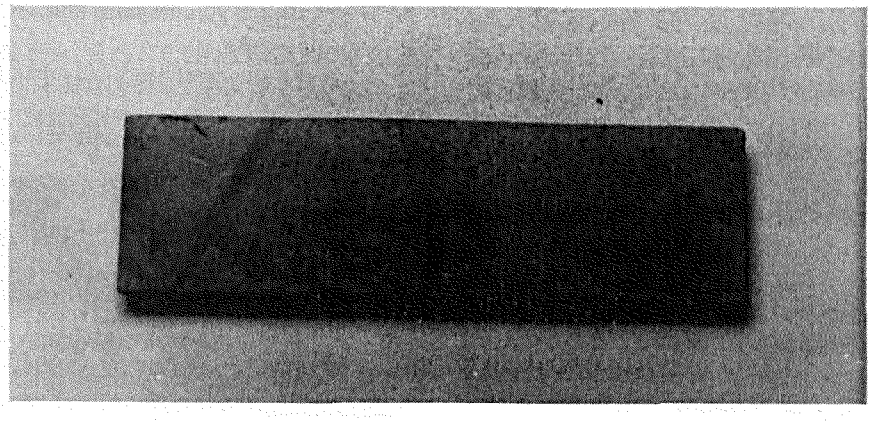

Figure 23. Preflawed specimen.

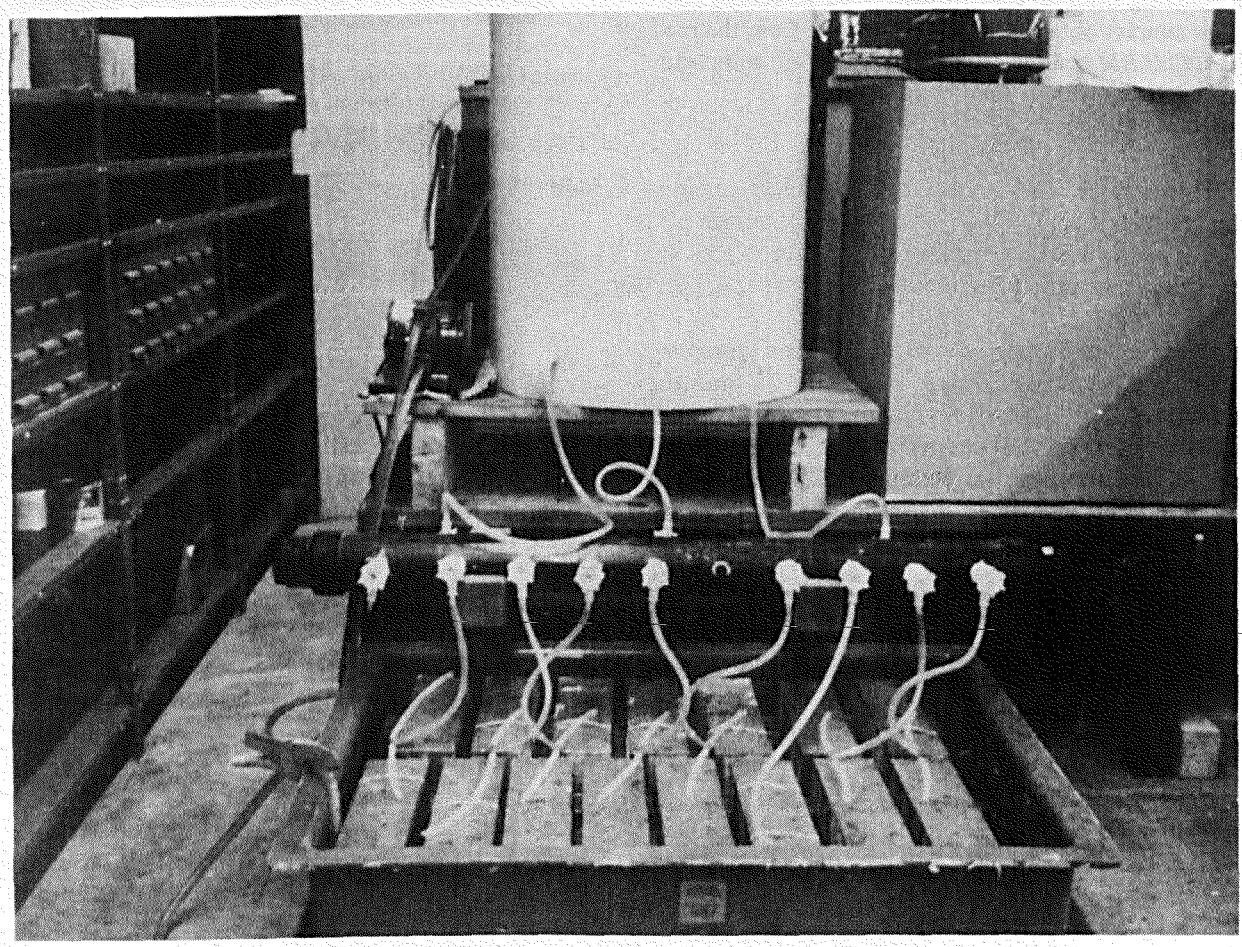

Figure 24. Wet-dry saltwater exposure apparatus.

The specimens were then exposed to a corrosive environment consisting of a flowing wet-dry aerated recirculating 3.5 percent sodium chloride aqueous solution. The solution was directed into the flaw of each preflawed specimen and over the surface of each unflawed specimen at a rate of about 24 oz (706 cm^3) per minute per specimen. The wet-dry cycle consisted of 8 hours wet and 16 hours dry every operational day. Figure 24 shows the exposure apparatus. The corrosive solution was periodically monitored for chloride concentration, oxygen concentration, pH, and temperature. Due to water losses from evaporation, periodically adding water to the main reservoir was necessary to maintain the 3.5 percent salt concentration.

Sets of one preflawed and one unflawed specimen were removed from the corrosive environment at different exposure times for evaluation of the extent of corrosion. Both specimen types were tested for third point loading flexural strength using standard test method ASTM C39-72.

Examination of crack interfaces and chloride permeability investigations were also performed. Preflawed specimen crack or flaw interfaces were examined for fibers which were not pulled out during the flexure test, but broke into two separate pieces, each of which remained imbedded in the concrete. These fibers were said to have lost their tensile-load-carrying capacity due to corrosion, since a noncorroded fiber of the type used would invariably be pulled out of the concrete matrix before undergoing a tensile failure. A relationship between time of exposure and percent loss of fibers was obtained for the preflawed specimens. The crack interfaces of the failed unflawed flexural specimens were examined for evidence of any fiber corro-

sion. The chloride permeability evaluation consisted of conducting chloride content tests[11] on powdered concrete samples obtained at various depths from the surface. Chloride content vs. depth curves were compared for specimens with various exposure times.

Results

The corrosive environment had an average oxygen content of 6.9 ppm (parts per million), an average pH of 9.1, and an average temperature of 73°F (23°C). Table 5 shows the properties of each mix.

The effect of the corrosive environment on three preflawed specimens is illustrated in Figures 25 through 29. Figures 25 through 27 show failed specimens tested after zero, 25, and 55 wet-dry cycles. Figure 28 is a plot of exposure time vs. percent fiber failure due to corrosion. This plot shows that over 90 percent of the fibers in the flaw failed due to corrosion after 40 days of wet-dry saltwater exposure. The rate of fiber failure was almost linear with increasing time, up to about 32 cycles. Beyond this time, the relationship became somewhat asymptotic to the 100th percentile limit.

Figure 29 shows the relationship between exposure time and flexural strength of the preflawed specimens. This curve is comparable to that of Figure 28, in that it is first linear and then becomes asymptotic to some limiting value. This finding is in keeping with theory, for as more and more fibers are overcome by corrosion, the strength dictated by ultimate load should approach the flexural strength supplied by the upper half of the preflawed cross section.

Figure 30 shows the effect of corrosion on the unflawed specimens. The flexural strength of the unflawed specimens continued to increase with increasing exposure times. It appears that the wet-dry saltwater environment allowed the concrete to continue to gain strength due to extended curing. Examination of the fracture surfaces of tested unflawed exposure specimens revealed no signs of corrosion of internal fibers. Figure 31 shows an uncorroded steel fiber located approximately 0.005 in. (0.13 mm) from the edge of the crack face of a specimen which had been tested after exposure to 90 wet-dry cycles.

Table 5
Mix Properties of Flawed and Unflawed Specimens

Mix	Slump, in. (cm)	Air Content, %	Unit Weight, lb/cu ft (kg/m^3)	Compressive Strength, lb/sq in. (N/cm^2)
Unflawed	3.5 (8.9)	4.5	146.4 (2345)	9324 (6429)
Flawed	3.75 (9.5)	5.4	144.0 (2307)	7873 (5428)

Figure 32 shows the results of the chloride permeability evaluation of the unflawed specimens. This curve shows the chloride concentration vs. depth relationship for specimens exposed for zero, 10, 30, and 90 wet-dry cycles. These curves indicate that the majority of the chloride permeation occurred in the first 30 cycles of exposure. After 90 cycles of exposure, little or no chloride was found at depths greater than 1 in. (25 mm) from the exposed concrete surface.

Discussion of Results

The results of this investigation indicate that after 40 applications of a wet-dry saltwater environment, 90 percent of the steel fibers which bridge a larger than hairline crack will undergo sufficient corrosion so that they will be of little or no benefit in maintaining integrity of the crack which they bridge. In contrast, continued hydration will cause uncracked steel fibrous concrete to experience a continual flexural strength increase during exposure to 90 applications of a wet-dry saltwater environment.

[11] H. A. Berman, "Determination of Chloride in Hardened Portland Cement Parts, Mortars, and Concrete," *ASTM Journal of Materials*, Vol 7, No. 3 (September 1972), pp 330-335.

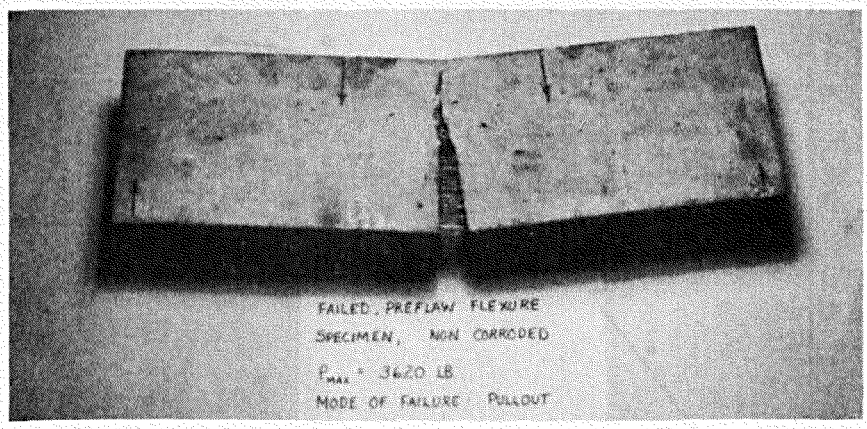

Figure 25. Tested preflawed specimen at zero wet-dry cycles.

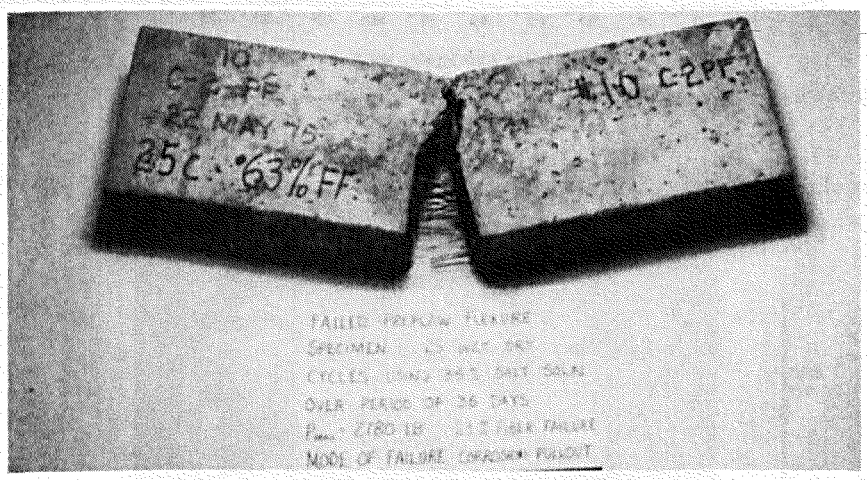

Figure 26. Tested preflawed specimen at 25 wet-dry cycles.

Figure 27. Tested preflawed specimen at 55 wet-dry cycles.

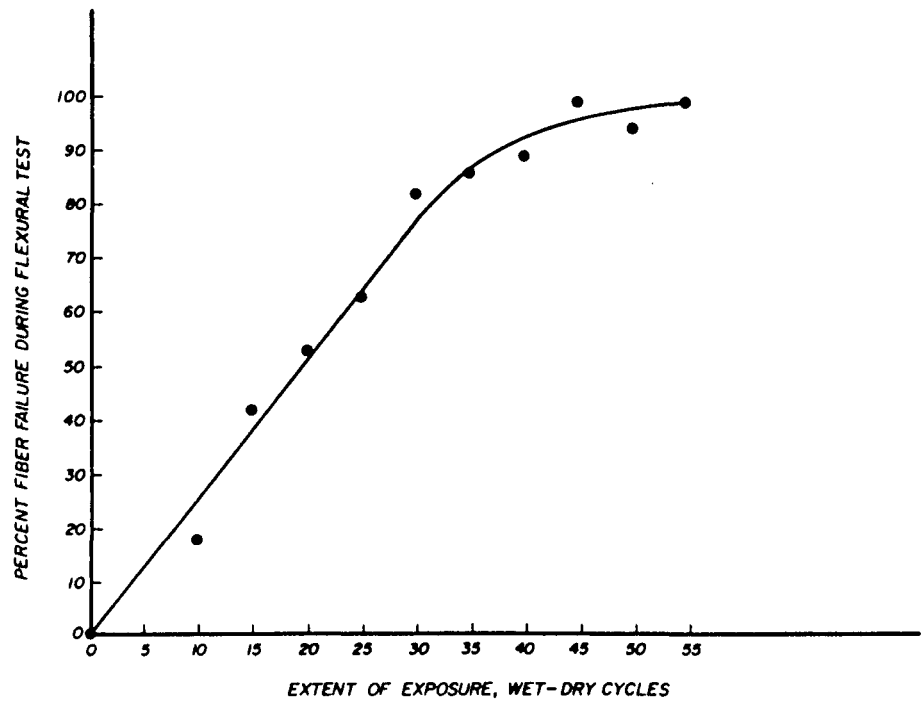

Figure 28. Loss of fiber integrity during flexural test for preflawed specimens of various degrees of exposure.

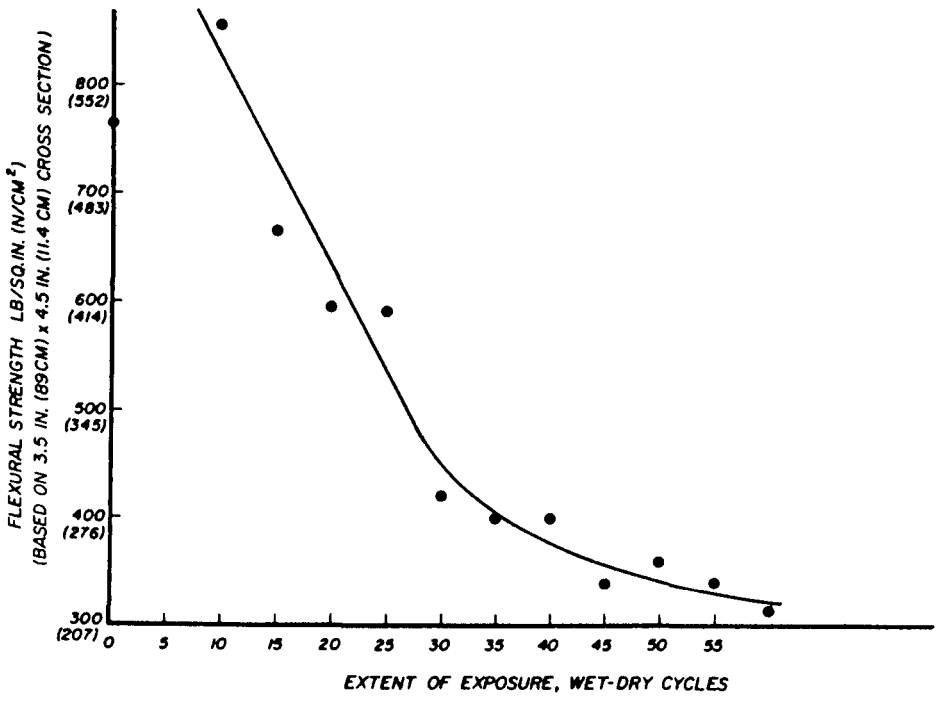

Figure 29. Loss of flexural strength of preflawed specimens at various degrees of exposure.

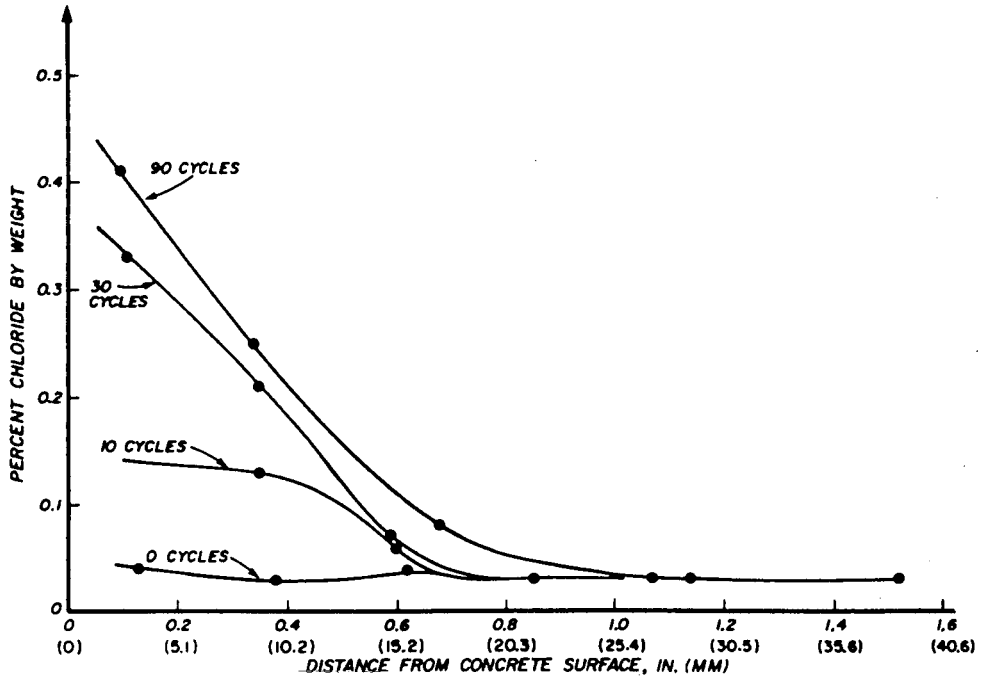

Figure 32. Chloride permeability of 1.5 percent steel fibrous concrete subjected to wet-dry saltwater environment.

5 EFFECT OF CORROSIVE ENVIRONMENT ON FATIGUE PERFORMANCE OF STEEL FIBROUS CONCRETE

Introduction

The investigations reported in Chapters 2 and 3 indicated that uncracked steel fibrous concrete is not adversely affected by a corrosive environment and that crack widths typical of steel fibrous concrete at or near ultimate flexural stress are not of sufficient size to render bridging fibers unprotected against available corrosive environments. These investigations have at least one limitation, however, in that their determinations apply to the behavior of unstressed fibrous concrete. In most applications, fibrous concrete is expected to undergo continual stress and stress fluctuations. For example, fibrous concrete used as a pavement is expected to resist prolonged fatigue loadings.

Corrosion is expected to have an effect on the fatigue behavior of fibrous concrete, particularly in the post-cracking stage. Since the opening and closing of a crack could facilitate the entry of corrosive substances, it appears that the working of a cracked or uncracked material could be an important factor in its corrosion behavior. Thus, the objective of the study described in this chapter is to determine the effect of fatigue on the corrosion behavior of steel fibrous concrete.

Procedure

The corrosion-fatigue behavior of steel fibrous concrete was studied using the concept of a semi-infinite beam on an elastic foundation. This method not only approximates the conditions under which fibrous concrete is expected to perform (e.g., pavements or building foundations), but it is also readily adaptable to the introduction of a corrosive environment. The method was also expected to provide conditions under which the post-cracking stage of fibrous concrete could be more thoroughly examined. The test apparatus consisted of a rubber pad and an electronically controlled hydraulic actuator located in a structural frame, as shown in Figure 33. The rubber pad was used to simulate an elastic foundation, and the hydraulic actuator was used to exert fatigue loadings.

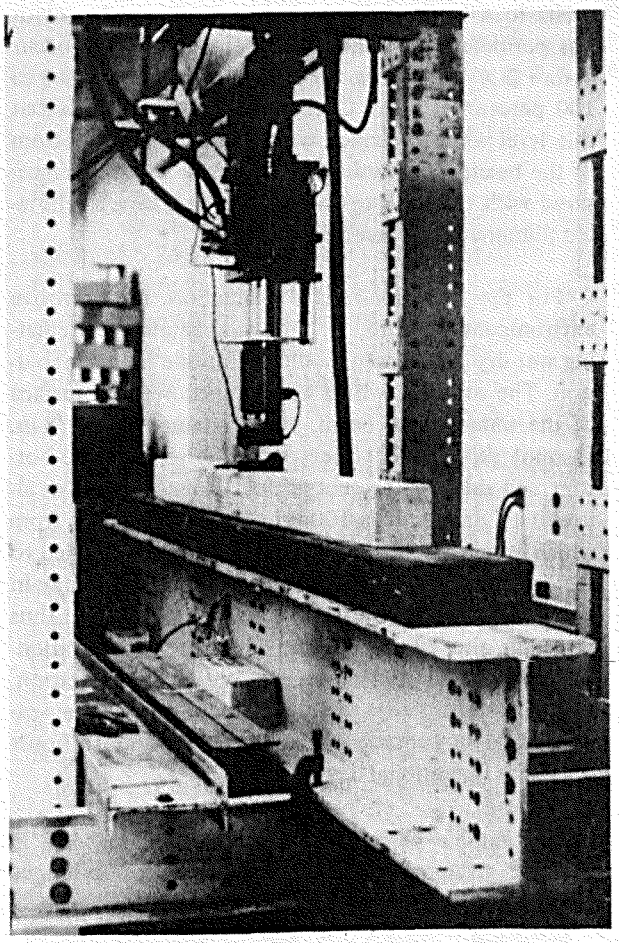

Figure 33. Beam on elastic foundation without corrosive environment.

The semi-infinite beams were made of 1.5 percent steel fibrous concrete and had 6 in. by 6 in. (152 mm X 152 mm) cross sections. The length of the beams was chosen such that the ratio of the end deflection to the center deflection was small. The minimum beam length for this condition to exist was determined from Eq 2.[12]

$$L = \frac{3.14}{\left(\frac{bk_0}{4EI}\right)^{1/4}} \qquad \text{[Eq 2]}$$

where L = beam length

b = beam width

k_0 = modulus of elasticity of the foundation

E = modulus of elasticity of the beam

I = moment of inertia of the beam.

The modulus of the rubber pad was to be 200 lb/cu in. (54 N/cm^3); that is, a 200 lb/sq in. (138 N/cm^3) pressure will produce a deflection of 1 in. (25.4 mm). This is a fairly average value for a soil plus base material arrangement. A 6-in. (152 mm) thick, type 70 SBR rubber pad was chosen for the elastic foundation in accordance with the selected modulus.

The modulus of elasticity of the 1.5 percent steel fibrous concrete was expected to be 4.5 X 10^6 lb/sq in. (3.1 X 10^{10} N/m^2).[13]

A minimum beam length of 9.34 ft (2.85 m) was determined using the appropriate values in Eq 2. A 12 ft X 12 in. X 6 in. (3.7 m X 305 mm X 152 mm) rubber pad was obtained; the foundation modulus of this pad for a 9 ft X 6 in. (2.7 m X 152 mm) rectangular contact area was experimentally determined to be 331 lb/cu in. (90 N/cm^3). Based on this figure, the minimum beam length was recalculated to be 8.24 ft (2.5 m). It was thus decided that 9 ft (2.7 m) would be a sufficiently long semi-infinite beam length for small end deflections.

A total of two semi-infinite and seven short 21 in. X 6 in. X 6 in. (533 mm X 152 mm X 152 mm) beams were fabricated along with two 6 in. X 12 in. (152 mm X 305 mm) standard compression cylinders. Table 3 gives the mix design. All specimens were moist cured. After 28 days of moist curing at standard conditions, two short beams and the two compression cylinders were removed for strength determinations. The remaining specimens were moist cured in excess of 60 days.

Upon removal from the curing room, the remaining specimens were divided into two groups. The first group, which contained one semi-infinite beam and two short companion beams, was used to evaluate the fatigue behavior without a corrosive environment. The second group, which included one semi-infinite beam and three short companion specimens, was used to evaluate the fatigue behavior in a corrosive environ-

[12] J. P. Den Hartog, *Advanced Strength of Materials* (McGraw-Hill Book Co., 1952); and M. Hetenyi, *Beams on Elastic Foundation*, (University of Michigan Press, 1946).

[13] G. R. Williamson, *Compression Characteristics and Structural Beam Design Analysis of Steel Fiber Reinforced Concrete*, Technical Report M-62/AD771908 (CERL, December 1973).

ment. The companion specimens were used to determine the stress-strain characteristics of that particular beam group prior to the start of fatigue or corrosion-fatigue exposure of the semi-infinite beam.

Strain gages were affixed at midspan to both sides of each semi-infinite beam near the top, middle, and bottom of the beam cross section. At least one of the companion specimens of each group was similarly equipped. The remaining companion specimens were equipped with strain gages at the bottom only. The stress-strain relationship of the companion specimens was determined by static third point flexural testing according to ASTM C39-72. The yield strain at the bottom set of strain gages was noted in each case. This point was taken as the first deviation from linearity of the stress-strain curve. Sixty-five percent of the yield stress was used as the maximum peak cyclic load, since a previous investigation[14] showed that failure would occur between 5,000 and 10,000 cycles for a 2 percent steel fibrous concrete with 0.017 in. (0.43 mm) diameter fibers. The minimum load applied was maintained at 100 lb (445 N) to prevent disengagement of the loading shoe from the beam loading point.

The strain corresponding to 65 percent of yield stress was obtained from stress-strain curves of the companion specimens. A concentrated cyclic load was applied to the semi-infinite beam at midspan until this strain level was obtained. This load was used as the peak cyclic load in the fatigue test.

The semi-infinite beams were subjected to fatigue loadings until either a crack occurred or 2×10^6 cycles were experienced. The fatigue loading rate was about 7 cycles per second in the noncorrosive condition. The cyclic rate was decreased for the corrosive condition, since corrosion is time-dependent. A cyclic rate of 2.1 cycles per second was used, since 2×10^6 cycles (a commonly accepted fatigue limit for concrete) would be reached at about 30 wet-dry cycles of corrosive environment. It was determined earlier (Figure 32) that at 30 wet-dry cycles, the majority of chloride permeation occurs, thus indicating the majority of corrosive solution permeation and subsequent attack.

If a crack occurred before 2×10^6 cycles, the beam was subjected to continued fatigue loadings at the same cyclic load level while maximum crack width growth was periodically monitored. If a crack did not occur before 2×10^6 cycles, the stress level was increased to 100 percent of yield. Cyclic loading was continued at this level while the crack width growth at the bottom of the beam was monitored. The crack width was measured with the peak cyclic load applied using a calibrated illuminated surface microscope.

For the corrosion-fatigue evaluation, the corrosive environment consisted of a flowing aerated recirculating wet-dry 3.5 percent sodium chloride aqueous solution. The solution, which was pumped over the surface of the semi-infinite beam, was contained by a 1/8-in. (3 mm) thick rubber sheet which enveloped the bottom and sides of the rubber pad. The solution was allowed to drain into a 100-gal (0.4 m^3) reservoir from which it was pumped (Figure 34). Water was added to the reservoir at a rate of 1.3 gal (5000 cm^3) per day in order to account for losses due to evaporation and thus maintain the proper sodium chloride concentration. The chloride concentration, pH, oxygen concentration, and temperature were periodically monitored. The wet-dry exposure consisted of 8 hours wet and 16 hours dry every operational day.

The fatigue behavior of the semi-infinite beam in the first group was compared to the corrosion-fatigue

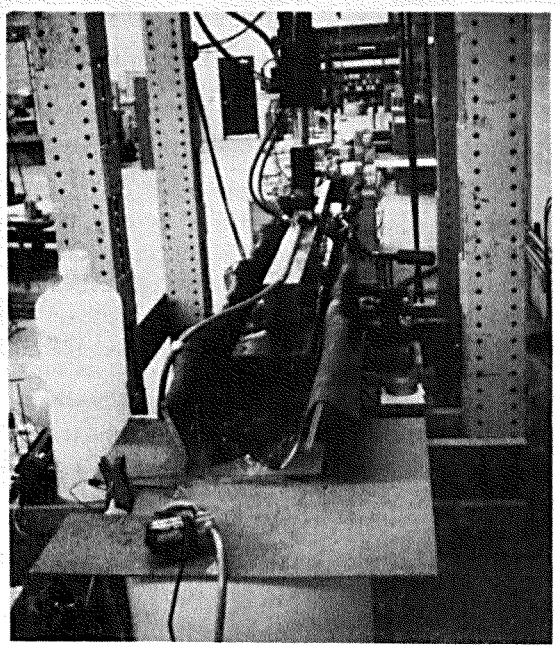

Figure 34. Beam on elastic foundation with corrosive environment.

[14] C. Ball, *The Fatigue Behavior of Steel-Fiber-Reinforced Concrete*, Master's Thesis (Clarkson College of Technology, October 1967).

behavior of the semi-infinite beam in the second group. The parameters considered to be important were cycles to first crack, crack width growth after the first crack had occurred, and condition of the beam at 2×10^6 cycles.

Results

The concrete used to fabricate specimens had a slump of 5.75 in. (146 mm), a unit weight of 143 lb/cu ft (2291 kg/m^3), and an air content of 5 percent. The 28-day strength of the specimens was 5836 lb/sq in. (4024 N/cm^2) compression and 1143 lb/sq in. (788 N/cm^2) ultimate flexural strength.

At the start of the fatigue exposure of the first semi-infinite beam, the ultimate flexural strength had increased to 1407 lb/sq in. (970 N/cm^2). The first crack strength at that time was 781 lb/sq in. (538 N/cm^2). The first crack strain was 0.000165 in./in. (.000 165 mm/mm) at the bottom strain gage. A load of 3000 lb (13 349 N) was required to produce 65 percent of first crack strain at the bottom strain gage of the semi-infinite beam on elastic foundation of the first group. This beam was subjected to 2×10^6 load cycles at 65 percent of first crack strain with no evidence of cracking. A load of 4500 lb (20 024 N) was required to produce 100 percent of first crack strain. The first crack was indirectly observed by the yielding of one of the strain gages near the bottom of the semi-infinite beam. Fatigue loadings were continued at the new peak cyclic load while the crack was located and monitored. Figure 35 shows the resulting maximum crack width vs. cycles relationship for the noncorrosive specimen. Fatigue loadings were discontinued at 2,552,840 cycles, since maximum crack opening measurements did not change between consecutive readings.

At the start of the corrosion-fatigue exposure of the second semi-infinite beam, the ultimate flexural strength was 1263 lb/sq in. (870 N/cm^2). The first crack strength was 764 lb/sq in. (527 N/cm^2), and the first crack strain was 0.000125 in./in. (.000 125 mm/mm). A load of 3300 lb (14 684 N) was required to produce 65 percent of first crack strain in the semi-infinite beam on elastic foundation. The semi-infinite beam on elastic foundation withstood 2×10^6 cycles of loading at 65 percent of first crack strain while being exposed to a total of 33 wet-dry cycles of the 3.5 percent sodium chloride environment. The corrosive solution had an average oxygen content of 6.8 ppm, an average pH of 8, 9, and an average temperature of 73°F (23°C). During this exposure, no evidence of cracking or other type of structural deterioration was found.

After 2×10^6 load cycles, a 4800 lb (21 359 N) load was required to produce 100 percent of first crack strain at the bottom gages. Load cycles were continued at this load level. A crack was immediately identified by the pumping of corrosive solution up from the bottom of the beam and out the sides of the crack. This pumping was caused by the opening and closing of the crack and capillary action. The crack width growth rate was very rapid compared to that of the semi-infinite beam not exposed to the corrosive environment. This crack width growth rate (Figure 36) was not considered to be a direct result of fiber corrosion; the crack width grew so quickly that the corrosive environment could not possibly have corroded the bridging fibers.

The loading characteristics of the beam were reexamined to determine the possible source of this rapid crack growth. Figure 37 shows a free body diagram of the beam. The force which is affected by the introduction of the saltwater environment is f, the foundation friction force. This force is most significant in affecting the post-cracking life of the beam because cyclic elongation is large at the crack due to opening and closing of the crack. This friction force holds the crack together. The lubricating effects of the saltwater between the beam and rubber pad greatly reduce this friction force. It is expected that this phenomenon caused rapid crack growth in the beam subjected to the corrosive environment.

Discussion of Results

The results of this investigation indicated that the corrosion behavior of uncracked 1.5 percent steel fibrous concrete appears to be unaffected by up to 2×10^6 fatigue loadings at 65 percent of first crack stress. The fatigue limit of 1.5 percent steel fibrous concrete used as a semi-infinite beam on an elastic foundation is at least 65 percent of first crack stress.

Since fiber deterioration was not the mode of crack growth, very little can be said about the post-cracking corrosion-fatigue behavior of steel fibrous concrete. The test apparatus used in this investigation was inadequate for evaluating the corrosion-fatigue behavior of cracked specimens due largely to the change in friction between the specimen and the elastic foundation caused by the wet corrosive environment.

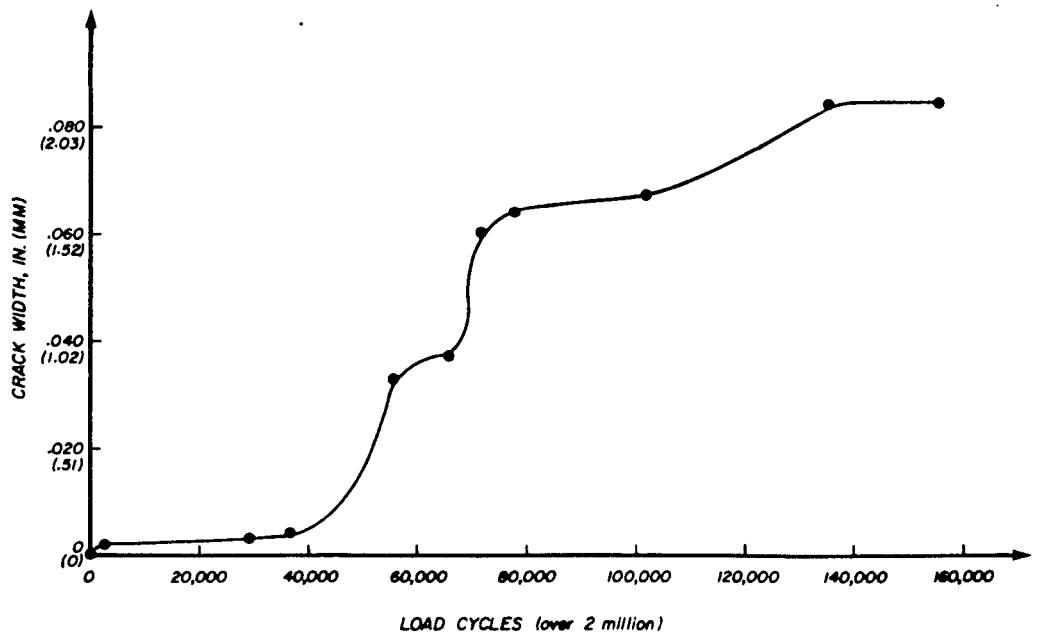

Figure 35. Load cycles vs. crack width for beam without corrosive environment.

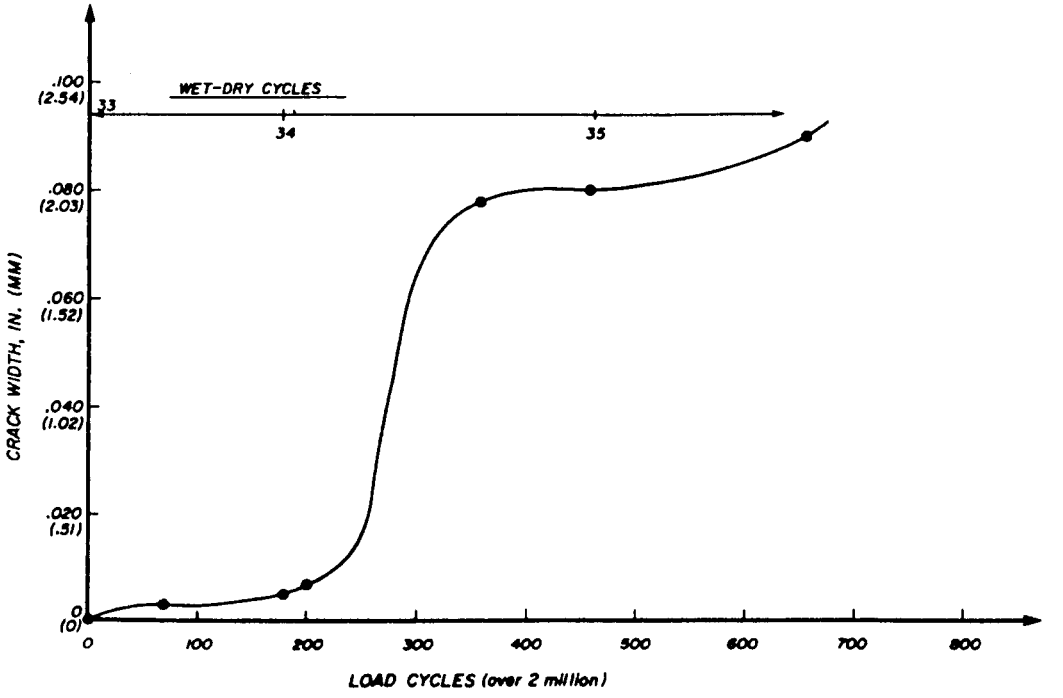

Figure 36. Load cycles vs. crack width for beam in corrosive environment.

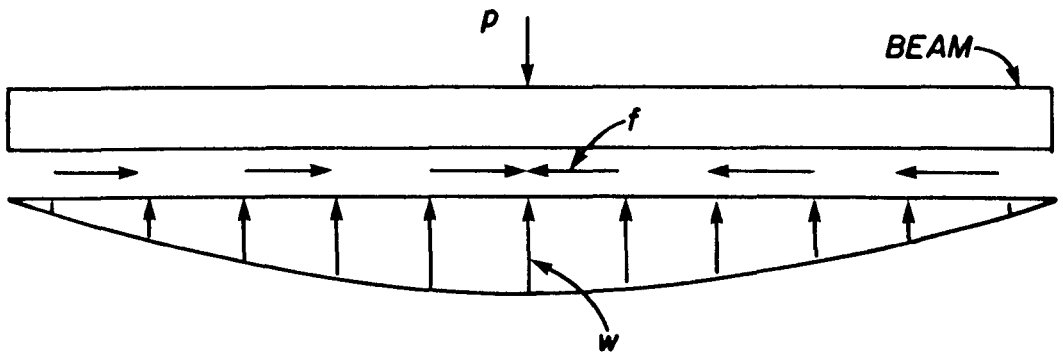

where p = the applied load

W = the compressive load per unit length exerted by the elastic foundation on the beam due to p and the beam weight

f = the horizontal friction forces exerted by the elastic foundation on the beam. Strain in the beam is imposed on the foundation by the friction between them. The magnitude of the force required to overcome friction is given by $f_o = f_u W$ where f_u is the coefficient of friction between the two interfaces.

Figure 37. Free body diagram of the semi-infinite beam on an elastic foundation.

6 CONCLUSIONS

Results of the investigations included in this report led to the following conclusions:

1. Interior steel fibers in good quality, air-entrained uncracked concrete do not corrode when exposed to a seawater environment for up to 1.5 years. Corrosion of fibers on or near the surface does occur, as evidenced by the brown surface staining seen in this study. This good quality fibrous concrete does not experience any undesirable strength changes in a seawater environment.

2. The strength of fibrous concrete containing either Kevlar or Fiberglas fibers is not significantly affected by a seawater environment.

3. Unworking hairline cracks which accompany attainment of ultimate strength in 1.5 percent steel fibrous concrete are not large enough to render the hairline-crack-bridging fibers unprotected against corrosive environments. The protective quality of interlocking crack interfaces appears to diminish at crack widths of greater than 0.01 in. (0.25 mm). When cracks of this size occur in 1.5 percent steel fibrous concrete, the ultimate flexural strength is expected to have already occurred; the remaining residual strength is approximately 58 percent of ultimate. As a result, cracks other than hairline in steel fibrous concrete should be sealed with a good quality joint sealer to maintain the integrity of the fibers.

4. Steel fibers bridging a crack and existing near the center of the crack face are less vulnerable to corrosion than bridging fibers near the edge of the crack face.

5. Corrosion failure of 90 percent of steel fibers bridging cracks larger than 0.01 in. (0.25 mm) is expected to occur after 40 applications of a wet-dry saltwater environment.

6. Continued hydration will cause uncracked steel fibrous concrete exposed to 90 applications of a wet-

dry saltwater environment to experience a continual flexural strength increase.

7. The corrosion behavior of uncracked 1.5 percent steel fibrous concrete is unaffected by up to 2×10^6 fatigue loadings at 65 percent of first crack stress.

8. The fatigue behavior of uncracked, good quality, air-entrained steel fibrous concrete at 65 percent of the first crack stress level is unaffected by exposure to a saltwater environment.

REFERENCES

Ball, C., *The Fatigue Behavior of Steel-Fiber-Reinforced Concrete*, Master's Thesis (Clarkson College of Technology, October 1967).

Berman, H. A., "Determination of Chloride in Hardened Portland Cement Parts, Mortars, and Concrete," *ASTM Journal of Materials*, Vol 7, No. 3 (September 1972), pp 330-335.

Biczok, I., *Concrete Corrosion and Concrete Protection* (Chemical Publishing Co., 1967).

Den Hartog, J. P., *Advanced Strength of Materials* (McGraw-Hill Book Co., 1952).

Erlin, B. and G. J. Verbeck, "Corrosion of Metals in Concrete–Needed Research," *Corrosion of Metals in Concrete*, Publication SP-49 American Concrete Institute [ACI], 1975), pp 39-46.

Hausman, D. A., "Steel Corrosion in Concrete," *Materials Protection* (November 1967), pp 19-22.

Hetenyi, M., *Beams on Elastic Foundation* (University of Michigan Press, 1946).

Lankard, D. R. and A. J. Walker, *Pavement Applications for Steel Fibrous Concrete*, presented at the ASCE Transportation Engineering Specialty Conference, Montreal, Canada, July 1974.

Shalon, R. and M. Raphael, "Influence of Sea Water on Corrosion of Reinforcement," *ACI Journal*, Proceedings, Vol 55, No. 12 (June 1959), pp 1251-1268.

Swamy, R. N. and P. S. Mangat, "A Theory for the Flexural Strength of Steel Fiber Reinforced Concrete," *Cement and Concrete Research*, Vol 4 (1974), pp 313-325.

Verbeck, G. J., "Mechanisms of Corrosion of Steel in Concrete," *Corrosion of Metals in Concrete*, Publication SP-49 (ACI, 1975), pp 21-38.

Williamson, G. R., *Compression Characteristics and Structural Beam Design Analysis of Steel Fiber Reinforced Concrete*, Technical Report M-62/AD-771908 (U. S. Army Construction Engineering Research Laboratory [CERL], December 1973).

Williamson, G. R. and B. H. Gray, *Technical Information Pamphlet on the Use of Fibrous Concrete*, Preliminary Report M-44/AD761077 (CERL, May 1973).

CERL DISTRIBUTION

Picatinny Arsenal
ATTN: SMUPA-VP3

US Army, Europe
ATTN: AEAEN

Director of Facilities Engineering
APO New York, NY 09827
APO Seattle, WA 98749

DARCOM STIT-EUR
APO New York 09710

USA Liaison Detachment
ATTN: Library
New York, NY 10007

US Military Academy
ATTN: Dept of Mechanics
ATTN: Library

Chief of Engineers
ATTN: DAEN-ASI-L (2)
ATTN: DAEN-FEE-A
ATTN: DAEN-FEB
ATTN: DAEN-FEZ-A
ATTN: DAEN-MCZ-S (2)
ATTN: DAEN-RDL
ATTN: DAEN-ZCP

ATTN: DAEN-PMS (12)
for forwarding to
National Defense Headquarters
Director General of Construction
Ottawa, Ontario K1AOK2
Canada

Canadian Forces Liaison Officer (4)
U.S. Army Mobility Equipment
Research and Development Command
Ft Belvoir, VA 22060

Div of Bldg Research
National Research Council
Montreal Road
Ottawa, Ontario, K1AOR6

Airports and Const. Services Dir.
Technical Information Reference
Centre
KAOL, Transport Canada Building
Place de Ville, Ottawa, Ontario
Canada, K1A ON8

British Liaison Officer (5)
U.S. Army Mobility Equipment
Research and Development Center
Ft Belvoir, VA 22060

Ft Belvoir, VA 22060
ATTN: ATSE-TD-TL (2)
ATTN: Learning Resources Center
ATTN: Kingman Bldg, Library

US Army Foreign Science &
Tech Center
ATTN: Charlottesville, VA 22901
ATTN: Far East Office

Ft Monroe, VA 23651
ATTN: ATEN
ATTN: ATEN-FE-BG (2)

Ft McPherson, GA 30330
ATTN: AFEN-FEB

Ft Lee, VA 23801
ATTN: DRXMC-D (2)

USA-CRREL

USA-WES
ATTN: Concrete Lab
ATTN: Soils & Pavements Lab
ATTN: Library

6th US Army
ATTN: AFKC-LG-E

I Corps (ROK/US) Group
ATTN: EACI-EN
APO San Francisco 96358

US Army Engineer District
New York
ATTN: Chief, Design Br
Buffalo
ATTN: Library
Saudi Arabia
ATTN: Library

US Army Engineer District
Pittsburgh
ATTN: Library
ATTN: ORPCD
ATTN: Chief, Engr Div
Philadelphia
ATTN: Library
ATTN: Chief, NAPEN-D
Baltimore
ATTN: Library
ATTN: Chief, Engr Div
Norfolk
ATTN: Library
ATTN: NAOEN-D
Huntington
ATTN: Library
ATTN: Chief, Engr Div
Wilmington
ATTN: Chief, SAWCO-C
Charleston
ATTN: Chief, Engr Div
Savannah
ATTN: Library
ATTN: Chief, SASAS-L
Jacksonville
ATTN: Library
ATTN: Const. Div
Mobile
ATTN: Library
ATTN: Chief, SAMEN-D
ATTN: Chief, SAMEN-F
Nashville
ATTN: Chief, ORNED-F
Memphis
ATTN: Chief, Const. Div
ATTN: Chief, LMMED-D
Vicksburg
ATTN: Chief, Engr Div
Louisville
ATTN: Chief, Engr Div
Detroit
ATTN: Library
ATTN: Chief, NCEED-T
St. Paul
ATTN: Chief, ED-D
ATTN: Chief, ED-F
Chicago
ATTN: Chief, NCCCO-C
ATTN: Chief, NCCED-F
Rock Island
ATTN: Library
ATTN: Chief, Engr Div
ATTN: Chief, NCRED-F
St. Louis
ATTN: Library
ATTN: Chief, ED-D
Kansas City
ATTN: Library (2)
ATTN: Chief, Engr Div
Omaha
ATTN: Chief, Engr Div
New Orleans
ATTN: Library (2)
ATTN: Chief, LMNED-DG
Little Rock
ATTN: Chief, Engr Div
Fort Worth
ATTN: Library
ATTN: SWFED-D
ATTN: SWFED-F
Galveston
ATTN: Chief, SWGAS-L
ATTN: Chief, SWGCO-C
ATTN: Chief, SWGED-DC
Albuquerque
ATTN: Library
ATTN: Chief, Engr Div
Los Angeles
ATTN: Library
ATTN: Chief, SPLED-F
San Francisco
ATTN: Chief, Engr Div
Sacramento
ATTN: Chief, SPKED-D
ATTN: Chief, SPKCO-C
Far East
ATTN: Chief, Engr Div
Japan
ATTN: Library
Portland
ATTN: Library
ATTN: Chief, DB-6
ATTN: Chief, FM-1
ATTN: Chief, FM-2
Seattle
ATTN: Chief, NPSCO
ATTN: Chief, NPSEN-FM
ATTN: Chief, EN-DB-ST

US Army Engineer District
Walla Walla
ATTN: Library
ATTN: Chief, Engr Div
Alaska
ATTN: Library
ATTN: NPADE-R

US Army Engineer Division
Europe
ATTN: Technical Library
New England
ATTN: Library
ATTN: Laboratory
ATTN: Chief, NEDCD
North Atlantic
ATTN: Library
ATTN: Chief, NADEN
South Atlantic
ATTN: Library
ATTN: Laboratory
ATTN: Chief, SADEN-TC
Huntsville
ATTN: Library (2)
ATTN: Chief, HNDED-CS
ATTN: Chief, HNDED-SR
Lower Mississippi
ATTN: Library
ATTN: Chief, LMVED-G
Ohio River
ATTN: Laboratory
ATTN: Chief, Engr Div
ATTN: Library
North Central
ATTN: Library
Missouri River
ATTN: Library (2)
ATTN: Chief, MRDED-G
ATTN: Laboratory
Southwestern
ATTN: Library
ATTN: Laboratory
ATTN: Chief, SWDED-TG
South Pacific
ATTN: Laboratory
Pacific Ocean
ATTN: Chief, Engr Div
ATTN: FM&S Branch
ATTN: Chief, PODED-D
North Pacific
ATTN: Laboratory
ATTN: Chief, Engr Div

Facilities Engineer
FORSCOM
Ft Devens, MA 01433
Ft McPherson, GA 30330
Ft Sam Houston, TX 78234
Ft Carson, CO 80913
Ft Campbell, KY 42223
Ft Hood, TX 76544
Ft Lewis, WA 98433
TRADOC
Ft Dix, NJ 08640
Ft Monroe, VA 23651
Ft Lee, VA 23801
Ft Gordon, GA 30905
Ft McClellan, AL 36201
Ft Knox, KY 40121
Ft Benjamin Harrison, IN 46216
Ft Leonard Wood, MO 65473
Ft Sill, OK 73503
Ft Bliss, TX 79916
HQ, 24th Inf, Ft Stewart, GA 31313
HQ, 1st Inf, Ft Riley, KS 66442
HQ, 5th Inf, Ft Polk, LA 71459
HQ, 7th Inf, Ft Ord, CA 93941
West Point, NY 10996
ATTN: MAEN-E
Ft Benning, GA 31905
ATTN: ATZB-FE-EP
ATTN: ATZB-FE-BG
CAC&FL
ATTN: DFAE (3)
Ft Leavenworth, KS 66027
AMC
Dugway, UT 84022
USACC
Ft Huachuca, AZ 85613

AF/PREEU
Bolling AFB, DC 20332

AF Civil Engr Center/XRL
Tyndall AFB, FL 32401

Little Rock AFB
ATTN: 314/DEEE/Mr. Gillham

Naval Facilities Engr Command
ATTN: Code 04
Alexandria, VA 22332

Port Hueneme, CA 93043
ATTN: Library (Code L08A)
ATTN: Morrell Library

Defense Documentation Center (12)

Washington, DC
ATTN: Bldg Research Advisory Board
ATTN: Library of Congress (2)
ATTN: Federal Aviation Administration
ATTN: Dept of Transportation Library
ATTN: Transportation Research Board

Engineering Societies Library
New York, NY 10017